

### **Reply to M.-Y. Lin's comments:**

We thank Meiyun Lin for her comments. Our responses are itemized below.

*“This is an interesting paper on the uncertainties in simulating STE in global models, especially with regard to global mean cross-tropopause flux. However, I believe your introduction and discussion sections will be more complete if you could place your study in the context of recent new findings on stratospheric influence on tropospheric ozone, particularly on high surface ozone events in the western United States [Langford et al., 2009; Lin et al., 2012]. A recent work by Lin et al. [2015, Nature Geoscience] shows that deep stratospheric intrusions can explain much of the year-to-year variability of springtime high surface ozone events measured at western US high-elevation sites during 1990-2012”.*

**Reply** – Thanks for the suggestion. We now state in the Introduction section that “Ozone is an important greenhouse gas, especially in the upper troposphere. It is a harmful pollutant near the surface where stratospheric ozone intrusions may make significant contributions (e.g., Lin et al., 2012, 2015; Langford et al., 2014).”

*“Large interannual variability in STE can confound the attribution of observed tropospheric ozone changes to human-induced emission trends [Lin et al., 2015; GRL]. There is great current interest to better understand the stratospheric influence on tropospheric ozone variability observed over the past few decades [e.g. Hess et al., 2015; Strode et al., 2015]. However, different models can do very differently in terms of STE and thus their simulation of tropospheric ozone interannual variability. Can you discuss if beryllium-7 can provide constraints on interannual variability of STE simulated in the model?”*

**Reply** – We now state in the last paragraph that “.....This can serve as a first-order assessment of cross-tropopause transport in the meteorological fields. With improved estimates of <sup>7</sup>Be production rates as well as their year-to-year variations, model multi-year <sup>7</sup>Be simulations together with long-term observations would provide useful constraints on the interannual variability of STE. While this study uses <sup>7</sup>Be alone, future modeling work will include using <sup>10</sup>Be/<sup>7</sup>Be, a more sensitive indicator of STE (Rehfeld and Heimann, 1995; Koch and Rind, 1998; Jordan et al., 2003).”

*“Most discussions on STE in your introduction section are based on the models with linoz or synoz chemistry, but there are recent model developments with interactive strat-trop chemistry at higher horizontal resolution (e.g., 50 km), which may be important to realistically simulate stratospheric intrusion events [e.g., Lin et al., 2012; Langford et al., 2014].”*

**Reply** – We now state in the Introduction section that “Observation-based estimates of STE fluxes of ozone into the troposphere are typically in the range of 400-600 Tg/year (Murphy and Fahey, 1994). Some global models are able to produce STE fluxes of ozone in this range (e.g., Olsen et al., 2004; Hsu et al., 2005; Hsu and Prather, 2009; Lin et al., 2012; Young et al., 2013; Skerlak et al., 2014).” and “.....Nevertheless, using Linoz (or full stratospheric chemistry) in global CTMs or chemistry-climate models that focus on the troposphere requires a realistic

model representation of net cross-tropopause total mass fluxes. In this context,  $^7\text{Be}$  tracer simulations may provide a simple way of evaluating cross-tropopause transport in these models.”

### **Reply to Referee #1’s comments:**

We thank Referee #1 for detailed and constructive comments. Our responses are itemized below.

*“GENERAL COMMENTS: Liu et al. study the impact of various meteorological data sets used in the Global Modeling Initiative (GMI) chemical transport model (CTM). In particular, they use a beryllium like aerosol tracer to assess stratosphere-troposphere exchange (STE) in the different meteorological fields. Since it is well known that all data fields have issues in realistically representing this process, constraints on STE in the model were made based on surface concentration measurements as well as on observed deposition fluxes of beryllium 7 ( $^7\text{Be}$ ). Moreover, the model results were compared with airborne measurements of  $^7\text{Be}$  and ozone in the upper troposphere and lower stratosphere. The observational constraints were further applied to other model simulations with the GFDL AM2 and GEOS-Chem, finally leading to the conclusion that these constraints result in a more reliable STE flux assessment.”*

*“Although research is conducted for a long time, STE is still a topic of intense debate. To assess the strength and location of STE properly is important for both air pollution studies as well as climate projections. Comparing available meteorological fields and assessing the strength of the errors of STE as well as the physical reason for these errors is a valuable contribution to further improve the quality of meteorological data sets. The paper is generally written in an understandable way, however, sometimes with the tendency to be a bit too descriptive. This finally results in a relatively long paper. The figures and tables are generally of good quality and presented along the discussion in the text. The applied methods are sound and the conclusions follow the discussion in the sections before. Overall, I support the publication of this study in ACP, after the following comments are addressed.”*

**Reply** – Thanks for the comments. Following Referee #2’s suggestion, this paper has been shortened.

*“DETAILED COMMENTS: 1) The introduction could benefit from some updated references. For instance, the paper from Riese et al. (2012), JGR, which shows the importance of assessing the concentrations of certain trace species in the UTLS (page 26134, line 8). The study of Skerlak et al (2014) presents climatology of STE and numbers on STE mass fluxes over the entire ERA-INTERIM time period (see paragraph on STE starting on page 26136, line 21). Maybe recent model comparison (from CCMI, ACCMIP, CMIP5) could also give further numbers.”*

**Reply** – We have included in the text the following references: Riese et al. (2012), Skerlak et al. (2014), and Young et al. (2013). We now state in the Introduction section that “Though correct representation of STE is essential for simulating  $^7\text{Be}$ , ozone and other trace species in the troposphere (e.g., Riese et al., 2012), large variations exist among models.” and “Observation-based estimates of STE fluxes of ozone into the troposphere are typically in the range of 400-600 Tg/year (Murphy and Fahey, 1994). Some global models are able to produce STE fluxes of

ozone in this range (e.g., Olsen et al., 2004; Hsu et al., 2005; Hsu and Prather, 2009; Lin et al., 2012; Young et al., 2013; Skerlak et al., 2014).” Reference: Young, P. J., et al.: Pre-industrial to end 21st century projections of tropospheric ozone from the Atmospheric Chemistry and Climate Model Intercomparison Project (ACCMIP), Atmos. Chem. Phys., 13, 2063-2090, doi:10.5194/acp-13-2063-2013, 2013.”

*“2) Regarding the model (section 2.1), what does “nearly full chemical treatment” mean? Could you specify the chemical mechanism a bit more in detail (NO<sub>x</sub>-VOC-O<sub>3</sub>, sulfur?). Furthermore, why are the aerosol and chemistry simulations conducted independently? “*

**Reply** – We have revised the text to “The GMI (<http://gmi.gsfc.nasa.gov>) CTM is a global 3-D composition model that includes a full treatment of both stratospheric and tropospheric photochemical and physical processes. It uses a 114-species chemical mechanism that combines the stratospheric mechanism of Douglass et al. (2004) with the tropospheric mechanism of Bey et al. (2001). The chemical mechanism includes both stratospheric and tropospheric heterogeneous reactions. Tropospheric aerosol (sulfate, dust, sea salt, organic carbon, and black carbon) fields are taken from the Goddard Chemistry, Aerosol, Radiation and Transport model (GOCART). Details of the model are described in Duncan et al. (2007, 2008), Strahan et al. (2007), and Considine et al. (2008).” Note that for the GMI full-chemistry simulation, tropospheric heterogeneous reactions and aerosol photochemical effects use monthly tropospheric aerosol fields from the GOCART model. For the radionuclide aerosol tracer (<sup>7</sup>Be) simulation, it does not involve interactions with chemistry and can therefore be conducted independent of full-chemistry simulations.

*“3) The horizontal resolution of the model simulation with 4°x5° is very coarse (section 2.1), especially since it is known that STE is very sensitive to the model resolution both in the vertical and horizontal. Is it possible to include at least one further simulation with one meteorological data set with an increased resolution and to discuss the differences? Is STE still overestimated in a high-resolution simulation? And consequently, is there a “threshold” resolution at which the observations are met satisfactory without applying further constraints. Also in section 6, wouldn’t it be more sensible to use a higher vertical resolution in the tropopause region in the AM2 simulations? Moreover, did I understand it right that always only full levels are either stratospheric or tropospheric or is there also an interpolation applied between two model (interface) layers?”*

**Reply** – (1). We discussed the differences in STE of <sup>7</sup>Be between a coarse resolution run (4°x5°) and an increased resolution run (2°x2.5°) in a previous study (Liu et al., 2001). As we stated in the text “The simulations presented here use a degraded horizontal resolution (4°x5°) for computational expediency. Degraded horizontal resolution slightly increases cross-tropopause transport (Liu et al., 2001). Nevertheless, our objective is to assess cross-tropopause transport in meteorological data sets at the resolution used to drive the model, not necessarily at the original or finer resolution.” (2). We believe that finding a “threshold” resolution is beyond the scope of this paper. (3). Following Referee #2’s suggestion, section 6 is now eliminated. (4). Yes, always only full levels are either stratospheric or tropospheric. There is no interpolation applied between two model layers.

“4) Could you please mention which advection scheme you are using and provide a reference? (page 26140, line 5)”

**Reply** – The reference is now added: “The model uses the flux-form semi-Lagrangian advection scheme of Lin and Rood (1996).....”. Reference: Lin, S. J. and Rood, R. B.: Multidimensional flux-form semi-Lagrangian transport schemes, Mon. Weather Rev., 124(9), 2046-2070, 1996.

“5) Beryllium attaches to the ambient aerosol and then it is treated as the aerosol. In the model the bulk mass is tracked. Is there an aerosol climatology provided to the model to assess the ambient aerosol. Or is the beryllium treated as a quasi-passive tracer with a fixed modal representation? If so, then it would be sensitive to give some additional meta information, such as molar mass (important for the dry deposition) and radius and sigma of the aerosol (usually important for the scavenging efficiency). Submicron particles can still have quite different scavenging efficiencies.”

**Reply** – We state in the Introduction section that “Beryllium-7 ..... After production, it attaches immediately to ubiquitous submicron aerosols in the ambient air. The fate of <sup>7</sup>Be then becomes that of those aerosols, which move with the air until scavenged by precipitation or deposited to the surface.” <sup>7</sup>Be is treated as a quasi-passive tracer, and the mass of <sup>7</sup>Be (not the mass of the ambient aerosol) is tracked. The molecular weight of <sup>7</sup>Be is 7 kg / kmole. Our scavenging scheme (Liu et al., 2001) does not take into account the submicron aerosol size-dependency of scavenging efficiencies.

“6) In section 2.2, it is mentioned that clouds, precipitation as well as convective transport are mainly responsible to obtain a good distribution of <sup>7</sup>Be. However, for STE often the strength and location of the subtropical jet is also crucial where quasi-isentropic exchange between tropospheric and stratospheric air masses can occur. Maybe it is worth thinking about to include a comparison of the location and strength of the jets between the different meteorological fields. The comparison in section 4 would also benefit from such a discussion. Is it possible to assess the error in the model deposition fluxes resulting from the over- and underestimation of precipitation? (page 26141, line 17 - 20)”

**Reply** – Good points. (1). We compared the location and strength of the subtropical jets in GEOS1-STRAT, fvGCM, and GEOS4-DAS (see below). It is indicated that the large differences in STE characteristics between GEOS1-STRAT and GEOS4-DAS (or fvGCM) is not explained by the slight differences in the location / strength of the subtropical jets in these meteorological fields.

<i>GEOS1-STRAT</i>	<i>latitude</i>	<i>pressure</i>	<i>maximum_wind</i>
<i>South Hemisphere:</i>	<i>30S</i>	<i>187hPa</i>	<i>31 m/s</i>
<i>North Hemisphere:</i>	<i>34N</i>	<i>187hPa</i>	<i>27 m/s</i>
<i>fvGCM</i>			
<i>South Hemisphere:</i>	<i>34S</i>	<i>193hPa</i>	<i>38 m/s</i>
<i>North Hemisphere:</i>	<i>38N</i>	<i>193hPa</i>	<i>28 m/s</i>
<i>GEOS4-DAS</i>			
<i>South Hemisphere:</i>	<i>30S</i>	<i>193hPa</i>	<i>31 m/s</i>
<i>North Hemisphere:</i>	<i>34N</i>	<i>193hPa</i>	<i>27 m/s</i>

(2). It is difficult to assess the error in the model deposition fluxes due to the bias in the model precipitation because such assessment would require information on the observed vertical distribution of precipitation.

*“7) In section 2.3: Following comment 5), how is the beryllium introduced into the model? Is it distributed evenly over the globe? Are there hot spots? Does the stratospheric aerosol have different parameters (size, sigma, etc.) than the aerosols in the upper troposphere? Moreover, and please correct me if I am wrong, but do I get it right that you use a constant  $^7\text{Be}$  production rate, which is, however, not so constant in reality (since it depends on the solar cycle). Thus, the constraints from the observations are based on a variable source strength, however, the model results are based on a constant source strength. Is it somehow possible to discuss this potential error between observations and model results a bit more in detail?”*

**Reply** – See our reply to comment 5) above. Now we state in section 2.3 that “The LP67 source is represented as a function of latitude and altitude (pressure) and does not vary with season (see Figure 1 of Koch et al., 1996)”. We also state at the beginning of section 2.5 that “We estimate an average solar year value simply by averaging the long-term records of  $^7\text{Be}$  observations multiplied by 0.72 to correct to the 1958 solar maximum source (Koch et al., 1996).”

*“8) Section 2.4 is difficult to read. However, the main points are not that difficult to understand. Maybe think about reducing the current content slightly and highlight the main points a bit more.”*

**Reply** – This section has been shortened, as also suggested by Referee #2.

*“9) In section 5 a comparison with other modeling studies is presented. It would also be helpful to provide some further numbers from studies of STE. Potentially, studies analyzing reanalysis data sets could be included, such as Skerlak et al. (2014). However, this could also be part of the introduction (see first comment).”*

**Reply** – See our reply to comment 1) above.

*“10) At the end of section 6 changes between results from model simulation are discussed. The differences are attributed to the various GEOS-DAS versions. Could you potentially list the major changes between the various data sets. Is this related to finer native resolution, different physical parameterizations, etc.? This might further help to understand the changes in the beryllium results. Why is cross tropopause transport slower in GEOS3-DAS? Is the jet structure different? Does the location of the tropopause vary strongly? Have there been significantly changes in the assimilation cycle?”*

**Reply** – Following Referee #2’s suggestion, we have eliminated section 6.

*“11) Why is the thermal tropopause used to calculate the tropospheric TOC in section 7? Would it not be more sensible to use the dynamical tropopause (based on a potential vorticity threshold, eg. 2 pvu). The temperature lapse rate tropopause is often not assumed to be the best marker*

*between stratosphere and troposphere, since there are situations where the thermal tropopause is not so well defined.”*

**Reply** – Point is well taken. On the other hand, we discuss in section 4 about the effect of different definitions of the tropopause by citing the work of Stajner et al. (2008): “Stajner et al. (2008) used four different definitions of the tropopause on the basis of temperature lapse rate (World Meteorological Organization or WMO definition), potential vorticity (PV), and isentropic surfaces or ozone surfaces. They found that the WMO tropopause was about 0.7-1 km (in the northern mid-latitude) or 0.5-1 km (in the tropics) higher than the ozone or PV determined tropopause.” The temperature lapse rate tropopause used here should not affect the conclusion of this study.

*“12) The discussion has often a quite descriptive character. An example is the second and third paragraph in section 4. STE is compared based on surface measurements of  $^7\text{Be}$ . It is mainly stated that there are differences between the model simulations but not what causes the differences, which are the main driving processes that cause the differences. I think the manuscript would benefit significantly, if such additional information could be provided directly.”*

**Reply** – See our reply to comment 6) above.

*“13) What is meant with satisfactory representation in line 7 on page 26157? Is this based on a certain (small) deviation from the expectation?”*

**Reply** – We meant “This suggests that models which utilize either of these fields could use the “Linoz” ozone scheme and expect reasonable representation of the stratospheric influence on tropospheric ozone on a global scale (i.e., STE fluxes of ozone within the range of observation-based estimates).” However, this section has been eliminated, following Referee#2’s suggestion.

#### **“TECHNICAL COMMENTS:**

*1) page 26142, line 6 : LP67 is not specified explicitly; 2) page 26146, line 5 : tropospheric → tropospheric; 3) page 26147, line 16: please define once SCM, either in the text or in a figure caption”*

**Reply** – Done.

*“4) page 26150, line 19: what is meant with standard simulation?”*

**Reply** – It means the reference simulation where no adjustment of  $^7\text{Be}$  cross-tropopause fluxes was made. To avoid confusion, we have removed “standard”.

*“5) page 26161, line 16: "to" is missing → helping "to" reduce ?”*

**Reply** – Both are OK.

*“6) page 26136, line 19: verus → versus”*

**Reply** – Corrected.

*“7) page 26150, line 10: middle latitudes → mid-latitudes”*

**Reply** – Changed.

*“8) page 26158, line 4 : greatest → largest”*

**Reply** – Changed.

*“9) Figure 2: maybe the convective mass fluxes could be compared to a high resolution convective mass flux of one reanalysis data set to see how large the difference are caused by the reduced resolution.”*

**Reply** – We believe that this is beyond the main scope of this study.

*“10) All colored latitude-height plots could benefit from a color bar (Figures 3, 6a, 7a, 9a, 10a, 11, 12)”*

**Reply** – Thanks for this suggestion. Color bars have been added for those figures.

*“11) Figures 11 and 12 could potentially be merged to one Figure 11 with two panels a,b, since they show the same content.”*

**Reply** – Following Referee #2’s suggestion, we have removed Figures 11 and 12 and relevant discussions.

*“12) In all line plots: at least in the printed version, the blue and purple lines are difficult to distinguish.”*

**Reply** – We have replotted all figures to improve their quality.

*“13) Caption of Figure 7 says ‘Same as Fig. 4....’, I think this should read ‘Same as Fig. 6...’.”*

**Reply** – Corrected.

*“14) Figure 15: a) and b) are mentioned in the caption but are not assigned to the two panels. Moreover, is it possible to add the zonal variability to  $\Delta\text{TOC}$  and  $\Delta^7\text{Be}$  in panel a), maybe by using gray contours. And is it further possible to add error bars to the best fit line in panel b)?”*

**Reply** – “a) and b)” are now added to the two panels. Error bars for  $\Delta\text{TOC}$  and  $\Delta^7\text{Be}$  are added in panel a). We choose to show in the legend the errors of the best-fitting parameters.

### **Reply to Referee #2's comments:**

We thank Referee #2 for detailed and constructive comments. Our responses are itemized below.

*“This manuscript uses the NASA Goddard Global Modeling Initiative (GMI) CTM, driven by 4 different meteorological data sets, to simulate the distribution of Be-7 in the atmosphere and its deposition to the surface. The meteorological data sets are known to differ significantly in their treatment of stratosphere to troposphere exchange STE (among other things); the authors hypothesize that Be-7 should provide a sensitive (and computationally inexpensive) test of how well STE is simulated in the models producing the meteorological field driving the CTM. A convincing case is made that compilations of observed Be-7 concentrations, coupled with prior work combining Be-7 and Sr-90, and long-term measurements of Be-7 deposition at a small number of mid latitude NH sites are adequate to assess how well the 4 different meteorological data sets implement STE within the GMI framework.”*

*“In later sections, the authors apply the Be-7 tests described above to several additional models, with additional meteorological data sets to reinforce the utility of Be-7 as a routine first-order test of how well any global model is simulating cross tropopause transport. Similarly, they drive the full chemistry version of GMI with 3 of the meteorological data sets used for the Be-7 simulations and compare simulated ozone to observations, finding that problems with STE identified in the Be-7 tests impact the simulated ozone fields in similar ways. In my opinions, these latter sections (6 and 7) are presented “in a rush” and do not add tremendous value to the overall story. I urge the authors to consider whether section 6 (and figures 11 and 12) could be deleted, and if section 7 could not be distilled to a few sentences discussing figure 15.”*

**Reply** – Thanks for the suggestions. We have deleted section 6 (including original Figures 11 and 12) but decided to keep section 7 to discuss the implications of different characteristics of cross-tropopause transport of <sup>7</sup>Be for stratospheric influence on tropospheric ozone in different meteorological fields.

*“Overall, this is a solid paper which does a thorough job making its main point, but feels too long. The motivation, approach, results and implications are clearly presented in most of the manuscript.”*

**Reply** – We have removed section 6 (see above).

*“Specific comments. Pg 7 line 31 and page 8 line 1. Given that previous GMI studies have used met fields from NCAR (CCM2 and CCM3) and found CCM2 to be best of one group tested, and CCM3 as good as its competition, why was the current version of CCM not included in this study?”*

**Reply** – The current version of CCM was not included in this study mainly because the four input meteorological data sets already provide adequate variability in cross-tropopause transport for the purpose of this study. On the other hand, CCM was not included in the later GMI simulations (e.g., X. Liu et al., 2007).



*“In section 2.3, the authors should provide some rationale for the decision to use the LP67 Be-7 formation rates, which have the highest global mean column production rate of the 3 options listed in lines 2 and 3 on page 9. A few sentences later in the same paragraph the authors state that a more recent formulation of Be-7 production rates (Usokin and Kovaltsov, 2008) “broadly agree with those of LP67 with slightly (about 25%) lower global production rate.” This would seem to imply that the global mean rate from Usokin and Kovaltsov is essentially identical to that suggested by Obrien et al., 1991, raising the question: if 2 approaches basically agree, why choose an older one with higher production rates? Later on in the paper there are several times that a positive bias is found when comparing model estimates to observed Be-7, which might partly be due to using too strong a source. For example, on page 13 lines 18-20 it is stated that the Usokin and Kovaltsov source would probably largely eliminate positive model bias in LS, presumably the Obrien source would also move things in the right direction, so why use LP67? Likewise on page 14 lines 2-5 and again in lines 19-22, it is stated that if observations had not been scaled down 28% the positive model biases would be much smaller, suggesting if the source in the model was 25% weaker the agreement would similarly improve.”*

**Reply** – Thanks for pointing this out. We have revised the text to “We use in the model the LP67 source for 1958 (solar maximum year) since it leads to the best simulation of aircraft <sup>7</sup>Be observations in the stratosphere where <sup>7</sup>Be concentrations are mainly determined by a balance between production and radioactive decay (Koch et al., 1996; Liu et al., 2001). Koch et al. (1996) previously found that the O'Brien (1991) source yields model <sup>7</sup>Be concentrations near the surface and in the stratosphere that are much lower than observed. The rates of <sup>7</sup>Be production reported more recently by Usoskin and Kovaltsov (2008) broadly agree with those of LP67 with slightly (about 25%) lower global production rate and will be tested in a separate model study.”

*“In section 2.4, the discussion of equations 2 through 7 is confusing to me, even after reading it many times. Can this be made both more clear, and probably shorter since in the end it turns out that relatively little time is spent in the discussion section on the scaling factor.”*

**Reply** – We have made it clearer and shorter in the revision.

*“Section 2.5 first sentence. While mathematically it is equivalent to either scale down long term averages of observed Be-7, or to scale up the production rate (by 28% in either case) to account for the fact that the production rates are produced for a year of solar maximum (production minimum) I have a philosophical preference for scaling the production rate up. As noted in section 2.3, there is significant disagreement between published estimates of the production rate (range is more than a factor of 2) so it would seem no one should object to adjusting these a little to facilitate model/data comparisons, while the data are the result of significant sustained effort to collect and analyze samples as accurately as possible.”*

**Reply** – While point is well taken, we use the <sup>7</sup>Be observational data compiled by Koch et al. (JGR 1996) and adopt their approach accordingly.

*“Section 4, discussion of Fig 6 (mainly on page 15, but also comments/questions about the figure and caption) Seems that you need to comment about the fact that according to the contours much of the lower strat in all 4 models shows strat fraction of Be-7 significantly less than 100%. Is this related to different definitions of the tropopause, or to seasonal movement of the tropopause vertically muddling the annual averages? Does not seem plausible that trop to strat transport is bringing that much tropospheric Be-7 into the LS, given the steep vertical gradient in concentrations. A more minor point, but first sentence in the figure caption says the plot shows “strat fraction of zonal mean tropospheric Be-7 concentrations”, but it clearly shows strat fraction in the full depth of the model atmosphere.”*

**Reply** – This is a good point. Now we state in the text that “The fractions of significantly less than 100% in the lower stratosphere in all four simulations reflect mainly the seasonal movement of the tropopause.” The figure caption is corrected to “Figure 6. (a). Stratospheric fraction (%) of annual zonal mean atmospheric <sup>7</sup>Be concentrations in the model simulations as a function of latitude and pressure...”.

*“Section 4, first paragraph on page 15, lines 9-15 and second paragraph lines 26-29. Here you strongly suggest that fvGCM and GEOS4 met fields are doing quite well with STE (clearly much better than the other 2). First paragraph ends by pointing out some very minor differences between the two “better” data sets, which are largely negated by the statement in the second paragraph. However later on you circle back and claim there are significant differences (e.g. pg 19, lines 8-11 and pg 20, lines 31-33), and claim that these were pointed out here in section 4. If you feel these differences need to be highlighted, make that point more strongly in this section.”*

**Reply** – Larger differences in the stratospheric fraction of <sup>7</sup>Be between fvGCM and GEOS-4 are seen in the free troposphere than at the surface. We have clarified this in the text: “However, GEOS4-DAS shows larger contributions from the stratosphere to the troposphere (especially the free troposphere) than fvGCM does by a few percent, consistent with the overestimated deposition fluxes at 20°N-40°N by GEOS4-DAS (Figure 5c).” and “.....On the other hand, it should be noted that the fvGCM and GEOS4-DAS simulations show results remarkably consistent with the DH85 constraint, suggesting that stratospheric influences on surface <sup>7</sup>Be concentrations in these two meteorological fields are reasonable.”

*“Technical comments Pg 5 line 32 representations.”*

**Reply** – Corrected.

*“Pg 8 line 1 delete “and”.*

**Reply** – Deleted.

*“Pg 8 line 12 Clouds and precipitation”*

**Reply** – Corrected.

*“Pg 8 lines 31-32 probably should note that Lal and Peters will be referred to as LP67 since you start doing that on page 9 (but not consistently). If you are going to use the acronym, probably should do it everywhere after pg 8”.*

**Reply** – Corrected.

*“Pg 14 line 6 deposition”*

**Reply** – Corrected.

*“Pg 15 lines 6-8 while it is true that GISS puts maximum strat fraction in the troposphere at high southern latitudes, both Fig 6a and 6b show that the fraction is nearly constant from just > 30 N all the way to the north pole”*

**Reply** – We now state in the text “With GISS II’, the stratospheric contribution to lower-tropospheric <sup>7</sup>Be concentrations peaks (30-40%) at southern high latitudes and remains nearly constant (30-35%) north of 30°N while it is quite small (<~10-20%) in the tropical middle and upper troposphere.”

*“Pg 15 lines 16-17 and the caption for Fig 6b. I think you are talking about strat fraction both in surface air, and in deposition, but as written it is ambiguous whether the dashed lines shows the total deposition, or the stratospheric fraction of total deposition”*

**Reply** – Now we state in the text “Figure 6b shows the stratospheric fraction (%) of annual zonal mean surface <sup>7</sup>Be concentrations and stratospheric fraction of annual zonal mean <sup>7</sup>Be total deposition fluxes (Bq/m<sup>2</sup>/yr) in the model simulations.” The caption for Fig. 6b has also been revised: “(b). Stratospheric fraction of annual zonal mean surface <sup>7</sup>Be concentrations (solid lines) and that of annual zonal mean <sup>7</sup>Be total deposition fluxes (dashed lines) in the model simulations as a function of latitude.”

*“In current draft, many of the figures are a little fuzzy. This is more distracting in line plots, but*

*also seems to degrade many of the maps. Specific examples: Figs. 1, 3 (especially contour labels), 4, 5, 6, 7, 8, 10, 13, 14.”*

**Reply** – We have re-plotted all the figures in the manuscript and converted the files to PNG format at high resolution. Color bars for contour plots have also been added, as suggested by Referee#1. We will also provide the original figures in postscript during the production process.

*“In caption for Fig 7. pretty sure it should be "Same as Fig 6" (not 4)”*

**Reply** – Corrected.

**Revised text with track changes**

**(next page)**

# Using beryllium-7 to assess cross-tropopause transport in global models

Hongyu Liu<sup>1</sup>, David B. Considine<sup>2,\*</sup>, Larry W. Horowitz<sup>3</sup>, James H. Crawford<sup>2</sup>, Jose M. Rodriguez<sup>4</sup>, Susan E. Strahan<sup>4,5</sup>, Megan R. Damon<sup>4,6</sup>, Stephen D. Steenrod<sup>4,5</sup>, Xiaojing Xu<sup>7</sup>, Jules Kouatchou<sup>4,6</sup>, Claire Carouge<sup>8,\*\*</sup>, and Robert M. Yantosca<sup>8</sup>

[1] National Institute of Aerospace, Hampton, VA, [USA](#)

[2] NASA Langley Research Center, Hampton, VA, [USA](#)

[3] NOAA Geophysical Fluid and Dynamics Laboratory, Princeton, NJ, [USA](#)

[4] NASA Goddard Space Flight Center, Greenbelt, MD, [USA](#)

[5] Universities Space Research Association, Columbia, MD, [USA](#)

[6] Sciencetific Systems and Applications, Inc., Lanham, MD, [USA](#)

[7] Sciencetific Systems and Applications, Inc., Hampton, VA, [USA](#)

[8] Harvard University, Cambridge, MA, [USA](#)

[\*] now at: NASA Headquarters, Washington, D.C., [USA](#)

[\*\*] now at: University of New South Wales, Sydney, Australia

*Atmospheric Chemistry and Physics*, [revised, March 2016](#)

**Correspondence to:** H. Liu ([Hongyu.Liu-1@nasa.gov](mailto:Hongyu.Liu-1@nasa.gov))

Chemistry and Dynamics Branch, Science Directorate

Mail Stop 401B, NASA Langley Research Center

Hampton, VA 23681

**Abstract.** We use the Global Modeling Initiative (GMI) modeling framework to assess the utility of cosmogenic beryllium-7 ( $^7\text{Be}$ ), a natural aerosol tracer, for evaluating cross-tropopause transport in global models. The GMI chemical transport model (CTM) was used to simulate atmospheric  $^7\text{Be}$  distributions using four different meteorological data sets (GEOS1-STRAT DAS, GISS II' GCM, fvGCM, and GEOS4-DAS), featuring significantly different stratosphere-troposphere exchange (STE) characteristics. The simulations were compared with the upper troposphere / lower stratosphere (UT/LS)  $^7\text{Be}$  climatology constructed from ~25 years of aircraft and balloon data, as well as climatological records of surface concentrations and deposition fluxes. Comparison of the fraction of surface air of stratospheric origin estimated from the  $^7\text{Be}$  simulations with observationally-derived estimates indicates excessive cross-tropopause transport at mid-latitudes ~~middle-latitudes~~ in simulations using GEOS1-STRAT and at high latitudes using GISS II' meteorological data. These simulations also overestimate  $^7\text{Be}$  deposition fluxes at mid-latitudes ~~middle-latitudes~~ (GEOS1-STRAT) and at high latitudes (GISS II'), respectively. We show that excessive cross-tropopause transport of  $^7\text{Be}$  corresponds to overestimated stratospheric contribution to tropospheric ozone. Our perspectives on STE in these meteorological fields based on  $^7\text{Be}$  simulations are consistent with previous modeling studies of tropospheric ozone using the same meteorological fields. ~~We further apply observational constraints to other global models including GFDL AM2 and GEOS-Chem (driven by GEOS3-DAS and GEOS5-DAS).~~ We conclude that the observational constraints for  $^7\text{Be}$  and observed  $^7\text{Be}$  total deposition fluxes can be used routinely as a first-order assessment of cross-tropopause transport in global models.

## 1 Introduction

Stratosphere-troposphere exchange (STE) of air masses and chemical species occurs at small-, synoptic and global-scales. It is typically associated with the occurrences of tropopause folding and cutoff cyclones and, more important, the global circulation of the atmosphere (Holton et al., 1995). While stratosphere-to-troposphere transport removes many chemical species from the stratosphere, it represents a significant source of ozone and other reactive species for the tropospheric chemical system (Stohl et al., 2003). Ozone is an important greenhouse gas, especially in the upper troposphere. It is a harmful pollutant near the surface where stratospheric ozone intrusions may make significant contributions (e.g., Lin et al., 2012, 2015; Langford et al., 2014). It is also the main precursor of hydroxyl radicals (OH) and thus

1 plays an essential role in the oxidizing capacity of the troposphere. The stratosphere may make  
2 significant contributions to In a warmer climate, the stratosphere may increase its contribution to  
3 tropospheric ozone levels due to a stronger residual circulation (Collin et al., 2003). Quantitative  
4 understanding and prediction of anthropogenic (versus natural) perturbations to tropospheric  
5 ozone require the use of global 3-D models; correctly representing the STE flux in these models  
6 is therefore critical. However, current models show large (30%) uncertainty in predicted STE  
7 fluxes of ozone (Stevenson et al., 2006). Here we use the Global Modeling Initiative (GMI)  
8 modeling framework (Douglass, et al., 1999; Rotman et al., 2001) to assess the utility of the  
9 aerosol tracer beryllium-7 ( $^7\text{Be}$ ) for evaluating cross-tropopause transport in global models.

10 Beryllium-7 has a half-life of 53.3 days and is produced by cosmic ray spallation reactions in  
11 the stratosphere and upper troposphere. After production, it attaches immediately to ubiquitous  
12 submicron aerosols in the ambient air. The fate of  $^7\text{Be}$  then becomes that of those aerosols, which  
13 move with the air until scavenged by precipitation or deposited to the surface.  $^7\text{Be}$  is a useful  
14 aerosol tracer for testing wet deposition processes in a global 3-D model and is often used in  
15 conjunction with the terrigenous  $^{210}\text{Pb}$  aerosol tracer, as wet deposition is its principal sink and its  
16 sources are relatively well known (e.g., Brost et al., 1991; Koch et al., 1996; Liu et al., 2001). On  
17 the other hand, because of its source at high altitudes and the large concentration vertical  
18 gradient, simulation of  $^7\text{Be}$  tests the model's capability to describe stratosphere-to-troposphere  
19 transport and subsidence in the troposphere (e.g., Liu et al., 2001; Allen et al., 2003).

20 Beryllium-7 has long been recognized as a tracer of downward transport from the  
21 stratosphere to the troposphere (e.g., Husain et al., 1977; Viezee and Singh, 1980; Sanak et al.,  
22 1985; Dibb et al., 1992, 1994; Rehfeld and Heimann, 1995). Husain et al. (1977) reported that  
23 pulses of high  $^7\text{Be}$  concentrations were often associated with air masses of stratospheric origin,  
24 as indicated by large potential vorticity. Viezee and Singh (1980) showed that the  $^7\text{Be}$   
25 concentrations over North America show strong positive correlations with the occurrence of  
26 tropopause folding events over several latitude belts.  $^7\text{Be}$  has also been combined with other  
27 radionuclides (e.g.,  $^{10}\text{Be}$ ,  $^{90}\text{Sr}$ ) as an indicator of transport of stratospheric air to the troposphere  
28 (Raisbeck et al., 1981; Rehfeld and Heimann, 1995; Koch and Rind, 1998; Dibb et al., 1994;  
29 Jordan et al., 2003; Zanis et al., 2003; Heikkila et al., 2008ab). Dutkiewicz and Husain (1985,  
30 hereafter referred to as DH85) analyzed  $^7\text{Be}$  and  $^{90}\text{Sr}$  concentrations measured simultaneously in  
31 samples from NASA's Global Atmospheric Sampling Program (GASP) and showed that on an  
32 annual basis the stratosphere contributed ~25% of the observed  $^7\text{Be}$  concentration at the northern  
33 mid-latitude surface (~40% during late spring but only 10% during fall).

Beryllium-7 is also a useful tracer for vertical mixing and subsidence in the troposphere. Feely et al. (1989) examined the factors that contribute to seasonal variations in  $^7\text{Be}$  concentrations in surface air. They found that the influences of variations both in the STE rate and in the tropospheric vertical mixing rate are evident in concentrations at most sites in ~~mid-latitudes~~ middle-latitudes. Convective transport carries surface air upward and brings down the  $^7\text{Be}$  at higher altitudes to the surface layer. This is also reflected by the  $^7\text{Be}/^{210}\text{Pb}$  ratio that peaks at the surface in summer when convective activity is at its maximum (Koch et al., 1996). On the other hand, despite the UT/LS source of  $^7\text{Be}$  and the continental surface source of  $^{222}\text{Rn}$  (precursor of  $^{210}\text{Pb}$ ),  $^7\text{Be}$  concentrations have been reported to be positively correlated with  $^{210}\text{Pb}$  concentrations, reflecting mixing of subsiding middle- and upper-tropospheric air with continental lower-tropospheric air (Li et al., 2002; Dibb, 2007).

A number of observational studies have demonstrated the feasibility of using  $^7\text{Be}$  to infer the contribution of ozone-rich stratospheric air to ozone concentrations at ground level (e.g., Husain et al., 1977; Tsutsumi et al., 1998; Helmig et al., 2007) and in the free troposphere (e.g., Johnson and Viezee, 1981; Prospero et al., 1995; Graustein and Turekian, 1996; Kritz et al., 1991; Dibb et al., 2003). These studies are usually based on the correlations between concurrent measurements of ozone and  $^7\text{Be}$  (as well as other tracers such as water vapor and calculated potential vorticity), with positive  $^7\text{Be}$ -ozone correlations indicating the presence of the upper-tropospheric or stratospheric air. For instance, Helmig et al. (2007) showed a year-round correlation of ozone with  $^7\text{Be}$  at Summit, Greenland and concluded that surface-layer photochemical ozone production does not appear to have a noticeable influence on surface ozone levels. However, it is important to note that under some circumstances the observed positive correlations of surface ozone with  $^7\text{Be}$  may simply reflect the common vertical trends of tropospheric  $^7\text{Be}$  and ozone and does not necessarily indicate the influence of stratospheric air (Li et al., 2002). Recent global modeling studies showed the models' capability to reproduce the observed  $^7\text{Be}$ -ozone relationships, providing useful constraints on the stratospheric (versus photochemical) contribution to tropospheric ozone in the model (Li et al., 2002; Allen et al., 2003; Liu et al., 2004).

Though correct representation of STE is essential for simulating  $^7\text{Be}$ , ozone and other trace species in the troposphere (e.g., Riese et al., 2012), large variations exist among models. Stevenson et al. (2006) reported the average STE flux of ozone from 26 models of  $552 \pm 168$  Tg/year. Observation-based estimates of STE fluxes of ozone into the troposphere are typically in the range of 400-600 Tg/year (Murphy and Fahey, 1994). Some global models are able to



1 produce STE fluxes of ozone in this range (e.g., Olsen et al., 2004; Hsu et al., 2005; Hsu and  
2 Prather, 2009; [Lin et al., 2012](#); [Young et al., 2013](#); [Skerlak et al., 2014](#)). For those models with  
3 too fast (or rarely, too slow) cross-tropopause transport of ozone, one way to overcome the  
4 difficulty is to use the Synoz (synthetic ozone) method (McLinden et al., 2000). The Synoz  
5 method involves constraining the global mean cross-tropopause ozone flux to match a prescribed  
6 value consistent with observations (e.g., Bey et al., 2001). But this method yields an unrealistic  
7 stratospheric ozone field and therefore does not allow for on-line calculations of total ozone  
8 columns and photolysis rates/heating rates (McLinden et al., 2000). By contrast, the other simple  
9 model for stratospheric ozone (linearized ozone or Linoz) developed by McLinden et al. enables  
10 these on-line calculations by linearizing the ozone tendency about the local ozone mixing ratio,  
11 temperature, and the overhead column ozone density. Linoz is computationally efficient and can  
12 be readily incorporated in climate models for long-term integrations. Nevertheless, using Linoz  
13 (or full stratospheric chemistry) in global CTMs or chemistry-climate models that focus on the  
14 troposphere requires a realistic model representation of net cross-tropopause total mass fluxes. In  
15 this context,  $^7\text{Be}$  tracer simulations may provide a simple way of evaluating cross-tropopause  
16 transport in these models.

17 The intermodel differences in the estimated intensity and frequency of STE have been  
18 attributed to different meteorological fields used to drive the models as well as different transport  
19 algorithms and chemistry processes (Cristofanelli et al., 2003). The GMI modeling framework  
20 facilitates the reduction of uncertainties of this kind. It is a modular CTM with the ability to  
21 incorporate different inputs and components (e.g., meteorological fields, emission inventories,  
22 chemical and microphysical mechanisms, and numerical schemes) that represent the different  
23 approaches of current models. One of the distinct features of the GMI CTM is the ability to be  
24 driven by different meteorological data sets (e.g., Douglass et al., 1999; Considine et al., 2005;  
25 Liu et al., 2007) while maintaining the same algorithms for transport, deposition, emission,  
26 chemistry and other pertinent processes. This allows us to isolate the uncertainties in the model  
27 simulations due to differences in the meteorological data sets alone. The number of factors that  
28 may contribute to differences in the simulations is thus reduced, as we previously showed using  
29 the GMI simulated  $^{222}\text{Rn}$  and  $^{210}\text{Pb}$  radionuclide tracers (Considine et al., 2005).

30 In this paper, we present simulations of atmospheric  $^7\text{Be}$  distributions with the GMI CTM  
31 driven by four different meteorological data sets, including output from GEOS1-STRAT, GISS  
32 II' GCM, fvGCM, and GEOS4-DAS, each featuring significantly different STE characteristics.  
33 The reader is referred to **Table 1** for a list of acronyms of models and their driving

meteorological data sets. We use here not only the meteorological fields that are well known to have reasonably good representations of STE (e.g., fvGCM) but also those with poor representations (e.g., GEOS1-STRAT). The variability in simulated STE allows us to examine and assess the utility of  $^7\text{Be}$  for evaluating STE in these (and other) global meteorological fields. We will illustrate the consequences of incorrect STE in terms of the simulation of tropospheric  $^7\text{Be}$  and show that  $^7\text{Be}$  concentrations and deposition fluxes may be used routinely as a first-order assessment for cross-tropopause transport in global models. We will discuss how the constraints on STE from  $^7\text{Be}$  are consistent with previous modeling studies of tropospheric ozone using the same meteorological fields. ~~We will also apply the  $^7\text{Be}$  tracer to assess cross-tropopause transport in GFDL-AM2-GCM and in other meteorological fields (GEOS3-DAS and GEOS5-DAS driving GEOS-Chem-CTM).~~

The remainder of this paper is organized as follows. Section 2 gives a brief description of the GMI model,  $^7\text{Be}$  source and cross-tropopause flux, and  $^7\text{Be}$  and ozone observational datasets used for evaluating the model. Section 3 evaluates model results with UT/LS and surface  $^7\text{Be}$  data. Section 4 assesses cross-tropopause transport of  $^7\text{Be}$  in different meteorological fields. Section 5 compares the results with previous modeling studies. ~~Section 6 assesses cross-tropopause transport of  $^7\text{Be}$  in a few other meteorological fields.~~ Section ~~6~~<sup>7</sup> discusses the implications for the impact of STE on tropospheric ozone, followed by summary and conclusions in Section ~~8~~<sup>7</sup>.

## 2 Model and data

### 2.1 GMI CTM

The GMI (<http://gmi.gsfc.nasa.gov>) CTM ~~(Combo-model)~~ is a global 3-D composition model that includes a ~~nearly~~ full treatment of both stratospheric and tropospheric photochemical and physical processes. It uses a 114-species chemical mechanism that combines the stratospheric mechanism of Douglass et al. (2004) with the tropospheric mechanism of Bey et al. (2001). The chemical mechanism includes both stratospheric and tropospheric heterogeneous reactions. Tropospheric aerosol (sulfate, dust, sea salt, organic carbon, and black carbon) fields are taken from the Goddard Chemistry, Aerosol, Radiation and Transport model (GOCART). Details of the model are described in Duncan et al. (2007, 2008), Strahan et al. (2007), and Considine et al. (2008). There is also a tropospheric version of the model that includes only tropospheric chemistry processes and uses the Synoz (synthetic ozone) scheme (McLinden et al.,

2000) to ensure a given value for the total flux of ozone into the troposphere. The latter adopts a cross-tropopause ozone flux of about 530-590 Tg/year (Stevenson et al., 2006). In this study, we simulate  $^7\text{Be}$  using the GMI CTM without chemistry, similar to the Considine et al. (2005) study that simulated the radionuclides  $^{222}\text{Rn}$  and  $^{210}\text{Pb}$ . We use both the full-chemistry CTM and the tropospheric version of the model for ozone simulations.

The simulations presented in this paper differ only in the meteorological data used to drive the model. The four input meteorological data sets are from: (1). the Goddard Space Flight Center Data Assimilation Office (now Global Modeling and Assimilation Office or GMAO) GEOS1-STRAT data assimilation system (GEOS1-STRAT DAS, March 1997 - February 1998), (2). GISS II' GCM (Rind and Lerner, 1996), (3). the GMAO finite-volume GCM (fvGCM), and (4). GEOS4-DAS (February 2004 – January 2005). The GISS II' GCM data set is used for  $^7\text{Be}$  simulations only. The two GCM data sets are intended to represent not any particular year but the contemporary climatological state of the Earth's atmosphere. Note that these data sets do not reflect the state-of-the-art, especially the first two. However, the choices are on purpose in order to see how a meteorological input with a poor representation of cross-tropopause transport affects the simulated tropospheric  $^7\text{Be}$ . Vertical levels, top pressure, near-tropopause resolution, and bottom layer depth for each data set are listed in **Table 2**. The simulations presented here use a degraded horizontal resolution ( $4^\circ \times 5^\circ$ ) for computational expediency. Degraded horizontal resolution slightly increases cross-tropopause transport (Liu et al., 2001). Nevertheless, our objective is to assess cross-tropopause transport in meteorological data sets at the resolution used to drive the model, not necessarily at the original or finer resolution.

The model uses the flux-form semi-Lagrangian advection scheme [of Lin and Rood \(1996\)](#) and a convective transport algorithm adapted from the CONVTRAN routine in the NCAR CCM3 physics package. The wet deposition scheme is that of Liu et al. (2001) and includes scavenging in wet convective updrafts, and first-order rainout and washout from both convective anvils and large-scale precipitation. The gravitational settling effect of cloud ice particles included in Liu et al. (2001) is not considered here. Dry deposition of  $^7\text{Be}$  aerosols is computed using the resistance-in-series approach. The model tracks the bulk  $^7\text{Be}$  aerosol mass. For  $^7\text{Be}$  simulations, each simulation was run for six years, recycling the meteorological data for each year of the simulation; we use the sixth year output for analysis. For ozone simulations, the model was spun up for 10 years to remove the effect of initial conditions. Interannual variability in STE of  $^7\text{Be}$  is not shown in this paper. However, model simulations driven by multi-year outputs from fvGCM (1994-1998) indicate that such interannual variability is much smaller than

the differences due to using different meteorological data sets and does not affect the conclusions of this study.

The GMI CTM has been used previously to study the sensitivities of model simulations to different sets of meteorological input. Douglass et al. (1999) used chemical tracers in the GMI framework to assess three meteorological data sets, i.e., the NCAR Community Climate Model (CCM2), GEOS1-STRAT, and GISS II' GCM. They concluded that overall, CCM2 provides the best representation of the stratosphere. Considine et al. (2005) used the GMI model to simulate the radionuclides  $^{222}\text{Rn}$  and  $^{210}\text{Pb}$  using three different sets of meteorological inputs (GEOS1-STRAT, GISS II', and CCM3) and to characterize the variability occurring in their simulations. Overall no simulation was found to be superior to the others when compared with the climatological observations of these radionuclides. The role played by convective transport and scavenging was found to differ substantially among the three meteorological data sets. Liu et al. (2007) analyzed and quantified the differences and uncertainties in GMI aerosol simulations solely due to different meteorological fields (GEOS1-STRAT, GISS II' GCM, and fvGCM). They suggested that the differences in the precipitation, convective mass flux, and horizontal advection from the three meteorological data sets explain much of the large discrepancies in the model-calculated aerosol concentrations.

## 2.2 Comparison of cloud and precipitation fields between meteorological data sets

Clouds and precipitation play a critical role in the transport and scavenging of  $^7\text{Be}$  aerosols and thus in determining the lifetime, burden, and distribution of  $^7\text{Be}$  in the troposphere. **Figure 1** and **Figure 2** compare the annual surface total precipitation and convective mass fluxes in the GEOS1-STRAT, GISS II' GCM, fvGCM and GEOS4-DAS meteorological data sets, respectively, following Liu et al. (2007). Also shown in **Figure 1** is the satellite climatology of surface total precipitation (1979-2009) from the Global Precipitation Climatology Project (GPCP) (Adler et al., 2003). The global mean precipitation rates are 1.9, 2.2, 2.6, 2.3 and 2.2 mm day<sup>-1</sup> for GEOS1-STRAT, GISS II' GCM, fvGCM, GEOS4-DAS and GPCP, respectively, with lightest precipitation in GEOS1-STRAT and heaviest in fvGCM. Compared to GPCP, GEOS1-STRAT and GEOS4-DAS significantly underestimate the precipitation in the mid-latitude storm track regions, while GISS II' GCM, fvGCM and GEOS4-DAS largely overestimate the observations in the tropics or subtropics. GISS II' GCM also underestimates the precipitation south of 50°S and north of 40°N. There are significant differences in the convective mass fluxes

among the four meteorological data sets (**Figure 2**). Consistent with the precipitation, GEOS1-STRAT shows the weakest convection except in the tropical middle and upper troposphere, whereas fvGCM features the strongest convection in the boundary layer at 30-60°S. The effects of the above differences in convection and precipitation between meteorological data sets on the results of this study will be examined through model sensitivity experiments.

### 2.3 <sup>7</sup>Be source

There is a large discrepancy in the published estimates of <sup>7</sup>Be production rates (Lal and Peters, 1967, referred to as LP67 hereafter; O'Brien et al., 1991; Masarik and Reedy, 1995; Masarik and Beer, 1999; Usoskin and Kovaltsov, 2008). Global mean column production rates over an average solar cycle range from 0.035 atoms cm<sup>-2</sup> s<sup>-1</sup> (Masarik and Beer, 1999), 0.063 atoms cm<sup>-2</sup> s<sup>-1</sup> (O'Brien et al., 1991), to 0.081 atoms cm<sup>-2</sup> s<sup>-1</sup> (LP67). The Masarik and Beer (1999) production function is smaller than other estimates by a factor of 2 or more. It may have underestimated the rate of <sup>7</sup>Be production and slightly overestimated changes in the production rate due to variations in geomagnetic and solar magnetic field strength (Koch et al., 2006; Field et al., 2006). We use in the model the LP67 source for 1958 (solar maximum year) since it leads to the best simulation of aircraft <sup>7</sup>Be observations in the stratosphere where <sup>7</sup>Be concentrations are mainly determined by a balance between production and radioactive decay (Koch et al., 1996; Liu et al., 2001). Koch et al. (1996) previously found that the O'Brien (1991) source yields model <sup>7</sup>Be concentrations near the surface and in the stratosphere that are much lower than observed. The rates of <sup>7</sup>Be production ~~recently~~ reported more recently by Usoskin and Kovaltsov (2008) broadly agree with those of LP67 with slightly (about 25%) lower global production rate and will be tested in a separate model study. ~~We use in the model the Lal and Peters (1967) source for 1958 (solar maximum year).~~ The LP67 source is represented as a function of latitude and altitude (pressure) and does not vary with season (see Figure 1 of Koch et al., 1996). About 2/3 of atmospheric <sup>7</sup>Be is generated in the stratosphere and 1/3 in the troposphere. The <sup>7</sup>Be production rate correlates inversely with solar activity. At higher solar activity, cosmic rays are deflected away from the solar system and the <sup>7</sup>Be production rate is thus lower.

### 2.4 Constraint on stratospheric contribution to <sup>7</sup>Be at the surface

Cross-tropopause transport is important for simulating <sup>7</sup>Be in the troposphere. A useful constraint on the stratospheric contribution to tropospheric <sup>7</sup>Be is DH85's analysis of the observed <sup>7</sup>Be/<sup>90</sup>Sr ratio in the stratosphere and <sup>90</sup>Sr concentrations at the surface. The presence of fissiogenic <sup>90</sup>Sr in the troposphere is due entirely to downward transport from the stratosphere, except for a few weeks right after a nuclear detonation. Both <sup>7</sup>Be and <sup>90</sup>Sr are associated with

submicron particles; their fates during transport from the stratosphere are expected to be similar (no differential removal is expected). The stratospheric  $^7\text{Be}$  component in surface air can therefore be determined as the product of the stratospheric  $^7\text{Be}/^{90}\text{Sr}$  ratio and the surface  $^{90}\text{Sr}$  concentration (DH85). By this procedure, DH85 showed that annually 23-27% (or about 25% on average) of the  $^7\text{Be}$  in surface air at northern mid-latitudes is of stratospheric origin. To use this constraint, we diagnose stratospheric contribution to  $^7\text{Be}$  concentrations in the troposphere by transporting separately in the model the  $^7\text{Be}$  produced in the stratosphere, as we previously applied in GEOS-Chem with GEOS1-DAS meteorological data (Liu et al., 2001). Since wet deposition removes both the stratospheric and tropospheric components of  $^7\text{Be}$  at the same rate within each model gridbox, the diagnosed stratospheric fraction of  $^7\text{Be}$  concentrations in the troposphere does not significantly depend on the rate of wet removal.

In the stratosphere, the production of  $^7\text{Be}$  (source) is balanced by radioactive decay and net STE fluxes of  $^7\text{Be}$  into the troposphere (sinks), i.e.,

$$\text{source } (^7\text{Be}) = \text{decay } (^7\text{Be}) + \text{STE } (^7\text{Be}). \quad (1)$$

~~Both terms on the right hand side are proportional to the stratospheric  $^7\text{Be}$  concentration, which is therefore proportional to the stratospheric  $^7\text{Be}$  source (the left hand side).~~ Since the time scale for downward transport from the stratosphere to troposphere ( $\sim 1$ -2 years) is much longer than that for radioactive decay (half-life 53.3 days), the radioactive decay term is much larger than the STE flux term. Nevertheless, the STE term would become more important for a model atmosphere where STE is too fast. ~~On the other hand, the STE fluxes of  $^7\text{Be}$  to the troposphere are proportional to the STE fluxes of air mass and the stratospheric  $^7\text{Be}$  concentrations.~~ ~~Therefore, f~~For the simulation of tropospheric (not stratospheric)  $^7\text{Be}$ , the stratospheric influx to the troposphere may be adjusted by artificially scaling down (in the case of excessive STE) or up (in the case of too slow STE) the stratospheric  $^7\text{Be}$  source. The extent to which  $^7\text{Be}$  cross-tropopause transport is excessive or too slow in the model can be indicated by a scaling factor A, which is defined as the ratio of model to ~~“real”~~ observed STE fluxes of  $^7\text{Be}$ . We derive the scaling factor A as follows.

According to the DH85 ~~observational~~ constraint, we have for the observations

$$[^7\text{Be}]_{\text{T,G}} / [^7\text{Be}]_{\text{S,G}} = (1-0.25)/0.25 = 3 \quad (2)$$

where the left-hand side denotes the ratio of the tropospheric ( $[^7\text{Be}]_{\text{T,G}}$ ) to stratospheric ( $[^7\text{Be}]_{\text{S,G}}$ ) component of annual mean  $^7\text{Be}$  concentrations in ground air at NH mid-latitudes. On the other hand, we have for a global model

$$[^7\text{Be}]_{\text{T,G}}' / [^7\text{Be}]_{\text{S,G}}' = (1-F)/F \quad (43)$$



where  $[^7\text{Be}]_{\text{T,G}}$  and  $[^7\text{Be}]_{\text{S,G}}$  are the *model* tropospheric and stratospheric components of annual mean  $^7\text{Be}$  concentrations in surface air at NH mid-latitudes, respectively, and  $F$  is the corresponding fraction of surface air of stratospheric origin in the model. ~~Our focus here is on the effects of cross-tropopause transport on surface  $^7\text{Be}$  concentrations in model simulations driven by different meteorological input data. The assumption (3) allows us to isolate such effects.~~

~~In the troposphere, the amount of the stratospheric  $^7\text{Be}$  tracer present is determined by a balance between downward transport from the stratosphere and its sink (dry and wet deposition and radioactive decay). The total sink is roughly in proportion to the average stratospheric  $^7\text{Be}$  tracer concentration in the troposphere; the latter is therefore about proportional to the STE fluxes. The scaling factor  $A$  may then be written as~~

$$A \equiv F_{\text{STE}}' / F_{\text{STE}} \approx [^7\text{Be}]_{\text{S,T}}' / [^7\text{Be}]_{\text{S,T}} \quad (5)$$

~~where  $F_{\text{STE}}'$  and  $F_{\text{STE}}$  are the STE fluxes of  $^7\text{Be}$  into the troposphere for the model and the observation, respectively;  $[^7\text{Be}]_{\text{S,T}}'$  and  $[^7\text{Be}]_{\text{S,T}}$  are the annual mean stratospheric  $^7\text{Be}$  tracer concentrations in the troposphere for the model and the observation, respectively. Assuming that~~  
If the model reasonably represents the vertical transport and wet scavenging processes in the troposphere, we have

$$[^7\text{Be}]_{\text{T,G}}' = [^7\text{Be}]_{\text{T,G}} \quad (4)$$

$$[^7\text{Be}]_{\text{S,T}}' / [^7\text{Be}]_{\text{S,G}}' \approx [^7\text{Be}]_{\text{S,T}} / [^7\text{Be}]_{\text{S,G}} \quad (6)$$

Combining equations (2)-(46), we obtain the scaling factor

$$A \approx [^7\text{Be}]_{\text{S,G}}' / [^7\text{Be}]_{\text{S,G}} \approx 3F / (1-F). \quad (75)$$

We will discuss the sensitivity of  $F$  and  $A$  to the assumptions with respect to convective transport and scavenging processes in Section 4. The validity of equation (75) will also be evaluated with actual model calculations in that section. Unless otherwise specified,  $^7\text{Be}$  cross-tropopause fluxes in the model calculations presented in this paper are not adjusted. However, we will use the scaling factor  $A$  as one of the metrics for comparing the STE characteristics of different meteorological data sets.

## 2.5 $^7\text{Be}$ and ozone observational data

$^7\text{Be}$ . We estimate an average solar year value simply by averaging the long-term records of  $^7\text{Be}$  observations multiplied by 0.72 to correct to the 1958 solar maximum source (Koch et al., 1996). The  $^7\text{Be}$  deposition flux observations are from the compilation of Koch et al. (1996) and there are about 25 northern mid-latitude sites with available long-term  $^7\text{Be}$  observations. The  $^7\text{Be}$  surface concentration observations are from the data archive of the US Department of Energy

(DOE) Environmental Measurements Laboratory (EML, now part of the Department of Homeland Security) Surface Air Sampling Program (SASP) beginning in the 1980's. We also use the long-term climatological data of  $^7\text{Be}$  concentrations in the UT/LS constructed from ~25 years of aircraft and balloon observations. Between the late 1950s and the early 1980s, EML collected tropospheric and stratospheric aircraft and balloon measurements of numerous radionuclides as part of the DOE High Altitude Sampling Program (HASP). The data was compiled into a database in 1997 by R. Leifer and N. Chan of EML, called RADionuclide DATaBase (RANDAB). The reader is referred to Considine et al. (2005) for a brief description of the RANDAB database. This database is available at the Oak Ridge National laboratory's Carbon Dioxide Information Analysis Center (<http://cdiac.esd.ornl.gov/ndps/db1019.html>).

*Ozone.* We use tropospheric ozone column (TOC) determined with the tropospheric ozone residual method by subtracting measurements of MLS stratospheric column ozone (SCO) from OMI total column ozone (Ziemke et al., 2006; URL: [http://acdb-ext.gsfc.nasa.gov/Data\\_services/cloud\\_slice](http://acdb-ext.gsfc.nasa.gov/Data_services/cloud_slice)) or using the TOMS and Solar Backscatter Ultraviolet (SBUV) combination (Fishman et al., 2003; URL: <http://science.larc.nasa.gov/TOR>). The OMI/MLS TOCs are from October 2004 - July 2008, and the TOMS/SBUV TOCs are from 1979-2005. We use climatological monthly average ozone profiles from 23 ozonesonde stations as constructed by Considine et al. (2008), based on Logan (1999) and Thompson et al. (2003). The ozonesonde data record is from 1985-2000 for extratropical stations, and from all available data prior to 2005 for tropical stations. The number of sondes at each station is adequate for defining monthly means used to evaluate the accuracy of the model results (Considine et al., 2008). Surface ozone data are taken from Logan (1999).

### 3 Model evaluation with UT/LS and surface $^7\text{Be}$ data

In this section, we present model results of  $^7\text{Be}$  simulations driven by four meteorological archives and evaluate them against long-term measurements at the surface and in the UT/LS. **Figure 3** shows the annual zonal mean concentrations (in units of millibecquerel per standard cubic meter or  $\text{mBq/SCM}^{-1}$ ) of  $^7\text{Be}$  in the four radionuclide simulations using GMI CTM. All four simulations overall show a similar pattern of tropospheric distribution. The highest concentrations are seen in the dry subsiding subtropics. Lowest  $^7\text{Be}$  concentrations in surface air are found in the Southern Hemisphere mid-latitudes owing to scavenging by frequent large-scale precipitation (**Figure 1**). Low  $^7\text{Be}$  concentrations are also associated with ITCZ, which is characterized by strong convergence and convective precipitation. It appears, however, that among all four simulations the GEOS1-STRAT simulation gives the highest concentrations in



the subtropics and the GISS simulation shows the highest concentrations in the high latitudes. This is partly attributed to the differences in the latitudinal distribution of total precipitations in these meteorological archives (**Figure 1**).

**Figure 4** compares four  $^7\text{Be}$  simulations in the upper troposphere / lower stratosphere (UT/LS) with climatological distributions constructed from the  $^7\text{Be}$  data contained in the RANDAB database, following Considine et al. (2005) who previously made a similar comparison for  $^{210}\text{Pb}$ . Model output are sampled at the months, longitudes, latitudes, and altitudes of the  $^7\text{Be}$  observations. **Figure 4a** compares the meridional distribution of  $^7\text{Be}$  measurements made in the 12-16km altitude range with the four GMI simulations. **Figure 4b** shows the same comparison, but for the 16-20km altitude range. The 12-16km (about 200-100hPa) range lies within the upper troposphere in the tropics and the lower stratosphere at mid to high latitudes. The 16-20km (about 100-50hPa) range lies within the stratosphere at all latitudes.

At 12-16km (**Figure 4a**), the observations indicate comparatively low tropical upper tropospheric values of  $\sim 35 \text{ mBq SCM}^{-1}$ , with increasing trends toward high latitudes. The distribution is nearly symmetric about the equator, with more observations available in NH high latitudes. This latitudinal distribution of  $^7\text{Be}$  concentrations reflects a larger production of  $^7\text{Be}$  in the lower stratosphere at high latitudes and precipitation scavenging associated with deep convection in the tropics. All four simulations capture the observations at 12-16 km reasonably well. The differences between the four simulated  $^7\text{Be}$  concentrations are comparable or smaller than the error limits.

At 16-20km (**Figure 4b**), the observations show a tropical minimum of  $\sim 150 \text{ mBq SCM}^{-1}$ , with increasing concentrations toward high latitudes in both hemispheres. In the tropics and the SH, the four  $^7\text{Be}$  simulations indicate small differences. In the NH, the four  $^7\text{Be}$  simulations reveal large differences and bracket the observations. In particular, the GMI/GEOS1-STRAT simulation gives the lowest  $^7\text{Be}$  concentrations among the four simulations and is lower than the observations. This appears to be due to excessive cross-tropopause transport in GEOS1-STRAT, as further discussed below. On the other hand, as we will also discuss later, the fvGCM and GEOS4-DAS meteorological fields have reasonable cross-tropopause transport. In the latter case, stratospheric  $^7\text{Be}$  concentrations are primarily determined by a balance between production and radioactive decay in the stratosphere. Therefore the slightly overestimated  $^7\text{Be}$  at 16-20km suggests a slightly overestimated global production rate of  $^7\text{Be}$  in the [Lal and Peters \(1967\)LP67](#) source. The Usoskin and Kovaltsov (2008) source, which is about 25% lower than the [Lal and](#)

[Peters \(1967\)LP67](#) source, would probably yield better agreements with the  $^7\text{Be}$  observations in the lower stratosphere.

**Figure 5a** compares the simulated and observed annual average concentrations of  $^7\text{Be}$  near the surface as a function of latitude. Observed data are from the EML SASP database and are averaged into  $10^\circ$  latitude bins. Observations from sites with elevation higher than 500m are not included because of uncertainties involved in sampling coarse-resolution models at high elevation sites. Model results are sampled at observation locations and month. **Figure 5b** shows the annual zonal mean surface  $^7\text{Be}$  concentrations in the model to indicate the global representativeness of the averages over the sampling sites. The observations indicate concentration maxima in the subtropics associated with subsidence and minima in the tropics. The tropical minimum reflects rapid scavenging within the ITCZ. Low  $^7\text{Be}$  concentrations are also observed at mid-latitudes due to efficient scavenging in the mid-latitude storm tracks. Latitudinal trends (i.e., minima and maxima) of  $^7\text{Be}$  concentrations are well simulated with all meteorological fields except GISS II'. The GMI/GISS simulation shows too high  $^7\text{Be}$  concentrations at high latitudes; this is because of the well-known excessive cross-tropopause transport at high latitudes in the GISS II' meteorological fields (e.g., Koch and Rind, 1998; McLinden et al., 2000; Shindell et al., 2003). The overall positive biases in all simulations are partly due to our correction of the long-term records of  $^7\text{Be}$  observations (by a factor of 0.72) to the 1958 solar maximum source (Section 2.5). We find that without this correction, the biases would be significantly reduced.

**Figure 5c** compares the model-simulated annual mean total deposition fluxes of  $^7\text{Be}$  at 25 northern mid-latitude sites from which long-term records of observations are available. The  $^7\text{Be}$  deposition flux observations are from the compilation of Koch et al. (1996), previously used in Liu et al. (2001). The data from individual sites are averaged over  $4^\circ$  latitude bins. The model is sampled at observation locations. **Figure 5d** shows the annual zonal mean total deposition fluxes of  $^7\text{Be}$  in the model to indicate the global representativeness of the sites. The observations show a maximum ( $\sim 2100 \text{ Bq/m}^2/\text{yr}$ ) in the subtropics ( $\sim 30^\circ\text{N}$ ) and the fluxes fall off with increasing latitude. The four  $^7\text{Be}$  simulations show large discrepancies especially in the subtropics ( $\sim 30^\circ\text{N}$ ). Overall, the GMI/fvGCM simulation agrees better with the magnitude of the observed fluxes while the GMI/GEOS4 simulation yields better latitudinal trends. GMI/GEOS4 simulates best the observations at the latitudes of  $45^\circ\text{N}$ - $60^\circ\text{N}$ , but overestimates the observations by  $\sim 50\%$  at  $20^\circ\text{N}$ - $40^\circ\text{N}$ . The GMI/GISS simulation overestimates the observations at higher latitudes ( $45^\circ\text{N}$ - $60^\circ\text{N}$ ) by a factor of  $\sim 2$ . The GMI/GEOS1-STRAT simulation overestimates the observed  $^7\text{Be}$

deposition fluxes at subtropical latitudes by up to a factor of 2.5 (30°N). As with the above model-observation comparison of surface <sup>7</sup>Be concentrations, the overall positive biases in model total deposition fluxes would be lower without the correction of <sup>7</sup>Be observations (by a factor of 0.72) to the 1958 solar maximum source (Section 2.5). However, we will show in the next section that these overestimated <sup>7</sup>Be deposition fluxes are largely due to model excessive cross-tropopause transport, especially with the GEOS1-STRAT and GISS II' meteorological fields.

#### 4 Assessment of cross-tropopause transport of <sup>7</sup>Be in different meteorological archives

The above results indicate different levels of success with four meteorological fields in reproducing long-term records of surface and UT/LS <sup>7</sup>Be concentrations as well as total deposition fluxes. In this section, we quantify the contribution of <sup>7</sup>Be produced in the stratosphere to tropospheric <sup>7</sup>Be concentrations and deposition fluxes, followed by an assessment of cross-tropopause transport of <sup>7</sup>Be in the meteorological fields used.

**Figure 6a** shows the stratospheric fraction (%) of annual zonal mean ~~tropospheric~~ atmospheric <sup>7</sup>Be concentrations (i.e., fraction of ~~tropospheric-atmospheric~~ <sup>7</sup>Be produced in the stratosphere) in the ~~standard~~-model simulations as a function of latitude and pressure. The fractions of significantly less than 100% in the lower stratosphere in all four simulations reflect mainly the seasonal movement of the tropopause. With GEOS1-STRAT, stratospheric contribution to lower-tropospheric <sup>7</sup>Be concentrations maximizes at 25-50°N (35-45%) and 25-40°S (30-35%). The tropical middle and upper troposphere show the minimum in stratospheric impact (<30%). With GISS II', the stratospheric contribution to lower-tropospheric <sup>7</sup>Be concentrations peaks (30-40%) at southern high latitudes and remains nearly constant (30-35%) north of 30°N while it is quite small (<~10-20%) in the tropical middle and upper troposphere. The strong gradients in the subtropics suggest that the tropics are strongly isolated from the mid-latitudes ~~middle latitudes~~ in the GISS II' meteorological field. fvGCM and GEOS4-DAS show similar pattern of stratospheric influence on the troposphere; both indicate maximum contribution from stratosphere near 30-35°N (~25%) and 25-30°S (~20-25%) in the lower troposphere. However, GEOS4-DAS shows larger contributions from the stratosphere to the troposphere (especially the free troposphere) than fvGCM does by a few percent, consistent with the overestimated deposition fluxes at 20°N-40°N by GEOS4-DAS (**Figure 5c**). The area of minimal stratospheric influence in the tropics is also narrower in GEOS4-DAS.

**Figure 6b** shows the stratospheric fraction (%) of annual zonal mean surface  $^7\text{Be}$  concentrations and that of annual zonal mean  $^7\text{Be}$  total deposition fluxes ( $\text{Bq}/\text{m}^2/\text{yr}$ ) in the model standard-simulations as a function of latitude. With all meteorological fields except GISS II', maximum stratospheric contribution to total deposition fluxes (versus surface  $^7\text{Be}$  concentrations) is shifted toward higher latitudes, reflecting scavenging by frequent mid-latitude precipitation and the dry subsidence in the subtropics. Stratospheric fractions of surface  $^7\text{Be}$  concentrations at NH mid-latitude are about 38% (GEOS1-STRAT), 33% (GISS II'), and 23-24% (fvGCM and GEOS4-DAS). As discussed in Section 2.4, the observed  $^7\text{Be}/^{90}\text{Sr}$  ratio suggests that 23-27% of the  $^7\text{Be}$  in surface air at northern mid-latitudes is of stratospheric origin (DH85). According to this constraint, cross-tropopause transport of  $^7\text{Be}$  and subsequent transport to the surface in the GEOS1-STRAT and GISS II' meteorological fields is excessive. On the other hand, it should be noted that the fvGCM and GEOS4-DAS simulations show results remarkably consistent with the DH85 constraint, suggesting that ~~cross-tropopause transport of~~ stratospheric influences on surface  $^7\text{Be}$  concentrations in these two meteorological fields are reasonable. However, DH85 did not provide constraints on latitudinal variation of stratospheric influence on surface  $^7\text{Be}$ . Of the four meteorological fields, GEOS1-STRAT, fvGCM and GEOS4-DAS show very similar latitudinal distribution of stratospheric influence at the surface (i.e., peak in the subtropics and valley in the tropics or polar regions). By contrast, GISS II' shows the largest impact of the stratosphere at high latitudes.

Similarly, as shown above, the model overestimates the long-term records of  $^7\text{Be}$  deposition flux observations at mid-latitudes ~~middle-latitudes~~ (and subtropics) with GEOS1-STRAT and at high latitudes with GISS II' (**Figure 5c**). Interestingly, the fvGCM (and to a lesser extent GEOS4-DAS) simulation yields  $^7\text{Be}$  deposition fluxes close to the observations. This suggests that the DH85 constraint and observed  $^7\text{Be}$  deposition fluxes are two complementary constraints on cross-tropopause transport of  $^7\text{Be}$ . We therefore use the DH85 constraint to assess the cross-tropopause transport of  $^7\text{Be}$  in the meteorological fields.

Using the approach described in Section 2.4 (i.e., reduced cross-tropopause transport flux by artificially scaling down the stratospheric  $^7\text{Be}$  source in the simulation of tropospheric  $^7\text{Be}$ ), we determine the scaling factors for GEOS1-STRAT and GISS to be 1.92 and 1.35, respectively. With the adjustment of  $^7\text{Be}$  cross-tropopause fluxes for GEOS1-STRAT and GISS, the model calculated stratospheric fraction of  $^7\text{Be}$  concentrations in surface air at NH mid-latitudes are indeed close to 25% (i.e., agree with the DH85 constraint) (**Figure 7**), thus supporting the validity of equation (75). With the adjustment, some simulations also simulate better surface  $^7\text{Be}$

1 concentrations and total deposition fluxes at the subtropics (GEOS1-STRAT) and at high  
2 latitudes (GISS II') (**Figure 8** vs. **Figure 5**). The improvement is clearer for total deposition  
3 fluxes than for surface concentrations. As discussed below, on a global scale total deposition  
4 fluxes are sensitive to STE fluxes of  $^7\text{Be}$  into the troposphere, while surface concentrations are  
5 principally dependent on the overall wet removal rate.

6 **Table 3** shows the annual average global budgets of tropospheric  $^7\text{Be}$  in the four GMI  
7 simulations. With an adjustment of  $^7\text{Be}$  cross-tropopause fluxes, the global burdens and  
8 residence times of tropospheric  $^7\text{Be}$  in GMI/GEOS1-STRAT and GMI/GISS are reduced. In  
9 GMI/GEOS1-STRAT the source and sink terms become much closer to that in fvGCM and  
10 GEOS4-DAS. A reduction of global  $^7\text{Be}$  STE fluxes of  $0.04 \text{ g d}^{-1}$  results in a decrease of total  
11 deposition fluxes of  $0.03 \text{ g d}^{-1}$  and radioactive decay of  $0.01 \text{ g d}^{-1}$ . In GMI/GISS the changes in  
12 the budget terms are relatively small due to the smaller adjustment of  $^7\text{Be}$  cross-tropopause  
13 fluxes. Nevertheless, a reduction of global  $^7\text{Be}$  STE fluxes of  $0.01 \text{ g d}^{-1}$  results in a decrease of  
14 total deposition fluxes of  $0.01 \text{ g d}^{-1}$ . These calculations indicate that globally the  $^7\text{Be}$  total  
15 deposition fluxes are sensitive to STE fluxes of  $^7\text{Be}$  into the troposphere.

16 The model calculated stratospheric fraction of  $^7\text{Be}$  in the troposphere may be sensitive to the  
17 model diagnosed location of the tropopause, for which there is some uncertainty. For instance,  
18 Stajner et al. (2008) used four different definitions of the tropopause on the basis of temperature  
19 lapse rate (World Meteorological Organization or WMO definition), potential vorticity (PV), and  
20 isentropic surfaces or ozone surfaces. They found that the WMO tropopause was about 0.7-1 km  
21 (in the northern mid-latitude) or 0.5-1 km (in the tropics) higher than the ozone or PV  
22 determined tropopause. We examine the sensitivity of model diagnosed stratospheric fraction of  
23 tropospheric  $^7\text{Be}$  concentrations to the location of tropopause (not shown) by lowering  
24 tropopause height by one model level (approximately 1.2 km, 1.7 km, 1.1 km, and 1.1 km for  
25 GEOS1-STRAT, GISS II', fvGCM and GEOS4-DAS, respectively). Results indicate that  
26 stratospheric fractions of surface  $^7\text{Be}$  concentrations increase by 5-10%, thus requiring larger  
27 adjustments of cross-tropopause transport of  $^7\text{Be}$  in the meteorological fields in order to meet the  
28 DH85 constraint. This also suggests that using the DH85 constraint requires relatively high  
29 vertical resolution near tropopause in the model.

30 While the model diagnosed stratospheric fraction of tropospheric  $^7\text{Be}$  concentrations is  
31 mainly determined by the STE processes in the UT/LS, it may also be sensitive to precipitation  
32 scavenging and convective transport in the troposphere. **Figure 9** shows the latitude-pressure  
33 cross sections of the differences in the stratospheric fraction (%) of annual zonal mean

1 tropospheric  $^7\text{Be}$  concentrations between the standard simulation and a simulation where  
2 precipitation scavenging is turned off. Also shown are the corresponding differences near the  
3 surface. The stratospheric fraction of tropospheric  $^7\text{Be}$  is found to be only weakly dependent on  
4 precipitation scavenging, with  $<5\%$  change in most of the troposphere and  $<2.5\%$  change near  
5 the mid-latitude surface. **Figure 10** shows a similar plot, except that convective transport and  
6 scavenging are turned off in the sensitivity simulation. Similarly, the stratospheric fraction of  
7 tropospheric  $^7\text{Be}$  is not sensitive to convective transport and scavenging processes, with  $<1\%$   
8 changes near the mid-latitude surface.

## 10 **5 Comparison with previous modeling studies**

11 In this section we compare the GMI CTM results for cross-tropopause transport of  $^7\text{Be}$  with  
12 previous modeling studies based on the same or similar meteorological fields.

13 Liu et al. (2001) found that STE flux of  $^7\text{Be}$  was overestimated with the GEOS1-STRAT  
14 fields in the GEOS-Chem model, consistent with this study using GMI CTM. However, Liu et al.  
15 (2001) found that the reduction required to match the DH85 constraint is a factor of 3.5 for the  
16 GEOS1-STRAT archive with  $4^\circ \times 5^\circ$  resolution, compared to a factor of 2.5 in the present study.  
17 The larger reduction in the former reflects the inclusion of ice particle gravitational settling  
18 effect, which results in increased transport from the upper to lower troposphere, as well as the  
19 inclusion of the diagnosed tropopause model layer as part of the stratosphere (versus the  
20 troposphere). Interestingly, when specifying ozone concentrations in the lower stratosphere  
21 (70hPa) and letting the model (GEOS-Chem) transport this ozone as an inert tracer into the  
22 troposphere, Bey et al. (2001) found a similar overestimate in an ozone simulation with the  
23 GEOS-1 data, as diagnosed by the simulation of tropospheric ozone concentrations at high  
24 latitudes in winter where transport from the stratosphere is a major source. This indicates that  
25 the simulation's deficiency in cross-tropopause transport as diagnosed using  $^7\text{Be}$  tracers has  
26 similar consequences for cross-tropopause transport of ozone.

27 Koch and Rind (1998) used a 31-layer version of the GISS GCM to simulate  $^7\text{Be}$  and  $^{10}\text{Be}$   
28 and used tropospheric  $^{10}\text{Be}/^7\text{Be}$  as indicator of STE. Based on limited observations, they  
29 suggested that leakage into the troposphere is somewhat excessive in the model, particularly at  
30 high latitudes. Using the GISS II' GCM, McLinden et al. (2000) found that a large fraction of the  
31 cross-tropopause transport of ozone occurs at the poles which is inconsistent with the current  
32 understanding of stratosphere-troposphere exchange, despite that the global stratosphere-  
33 troposphere exchange fluxes of ozone compare well with their best estimate of  $475 \pm 120$  Tg/year

1 based on measurements and tracer-tracer correlation. Shindell et al. (2003) presented an updated  
2 version of the GISS II' climate model which still overestimates ozone in the middle troposphere  
3 at high latitudes, likely reflecting deficiencies in the model's downward transport of stratospheric  
4 air. Our conclusions about cross-tropopause transport of  $^7\text{Be}$  in GISS II' in this work are  
5 consistent with these previous studies. Overestimated STE fluxes of  $^7\text{Be}$  as diagnosed in  
6 GMI/GISS based on the DH85 constraint simply reflect the incorrect latitudinal distribution of  
7 cross-tropopause transport, that is, too fast STE at higher latitudes and too slow STE at lower  
8 latitudes. The DH85 constraint was only applicable and applied for NH mid-latitude surface and  
9 thus does not provide constraint on the model global STE flux of  $^7\text{Be}$  if the latitudinal  
10 distribution of STE is incorrect.

11 The large-scale stratospheric transport (Brewer-Dobson circulation) in fvGCM has been  
12 shown to be realistic (Douglass et al., 2003) and mean age of stratospheric air is similar to  
13 observations (Strahan and Douglass, 2004; Douglass et al., 2008; Strahan et al., 2009). This  
14 suggests credible cross-tropopause transport of mass and ozone in fvGCM because the large-  
15 scale exchange between the stratosphere and troposphere is largely tied to the Brewer-Dobson  
16 circulation through the overworld wave driving (Holton et al., 1995; Olsen et al., 2004). Based  
17 on this finding, the meteorological data from fvGCM was used to drive GMI CTM by several  
18 authors to study tropospheric ozone. Considine et al. (2008) evaluated near-tropopause ozone  
19 distributions with ozonesonde data. Terao et al. (2008) examined the role of variability in the  
20 input of stratospheric ozone on the interannual variability of tropospheric ozone in the northern  
21 extratropics. Liang et al. (2009) investigated the impact of stratosphere-to-troposphere transport  
22 on tropospheric ozone and  $\text{NO}_x$  chemistry over the Arctic. By contrast, GEOS4-DAS tends to  
23 have too strong of a residual circulation, and the age of air is too young as compared to  
24 observations (Schoeberl et al., 2003; Schoeberl, 2004; Douglass et al., 2008). A GMI CTM  
25 simulation driven with the GEOS4-DAS meteorological fields showed the model's inadequacy  
26 in simulating upper-tropospheric ozone (Liang et al., 2009). These findings are consistent with  
27 what we illustrated in this study from a perspective of  $^7\text{Be}$  tracers. That is, GEOS4-DAS features  
28 larger impact of STE on the troposphere (especially UT) than fvGCM does, while the latter has  
29 more credible cross-tropopause transport as constrained by observed  $^7\text{Be}$  deposition fluxes  
30 (Figure 5c) and the DH85 criterion (Figure 6).

## 32 **6—Application to other meteorological fields**



1 In previous sections, we have established  $^7\text{Be}$  as a useful utility for testing the cross-  
2 tropopause transport in global models. In practical applications, such as the development and  
3 evaluations of new global models, the DH85 constraint may be used routinely as a first order  
4 assessment of cross tropopause transport. These models can be either online (e.g., GCMs) or  
5 offline (e.g., CTMs driven with archived meteorological data). In this section, we illustrate such  
6 applications by applying the DH85 constraint to assess cross tropopause transport of  $^7\text{Be}$  in a few  
7 other meteorological fields, including those from the GFDL global atmosphere model AM2,  
8 GEOS3-DAS and GEOS5-DAS. Model simulations are conducted with AM2 and GEOS-Chem  
9 CTM (driven by a series of GEOS-DAS meteorological data), respectively.

10 The GFDL coupled chemistry-climate model is developed by implementing a tropospheric  
11 chemistry package from the global MOZART-2 model (Horowitz et al., 2003) within the AM2  
12 climate model (GFDL GAMDT, 2004). Built on this framework, we have made the model  
13 capable of simulating both  $^{210}\text{Pb}$  and  $^7\text{Be}$  aerosol tracers by implementing their sources and  
14 sinks, i.e., dry and wet deposition, and radioactive decay (Liu et al., Lead 210 and beryllium-7  
15 simulations with the new GFDL global atmosphere model AM2, Technical Report, UCAR  
16 Visiting Scientist Program, Boulder, CO, May 2006). The model has  $2^\circ \times 2.5^\circ$  horizontal  
17 resolution with 24 vertical levels in a hybrid sigma/pressure coordinate with the interface at 250  
18 hPa. There are 19 levels in the troposphere, including 9 in the boundary layer. The upper  
19 troposphere has  $\sim 2\text{km}$  resolution. There are five levels in the stratosphere, with top level at about  
20 3 hPa. We use the Lal and Peters (1967)  $^7\text{Be}$  source for 1958, and the Harvard wet deposition  
21 scheme for the rainout (in cloud scavenging) and washout (below cloud scavenging) due to  
22 stratiform precipitation (Liu et al., 2001). Convective scavenging of aerosols was coupled with  
23 the Relaxed Arakawa-Schubert (RAS) cumulus parameterization. We conduct model integrations  
24 for six years (1982–1987) forced with observed sea surface temperature and use the year 1987  
25 for analysis. Interannual variability does not significantly affect our results.

26 When the model vertical grid level containing the tropopause is included as part of the  
27 troposphere, the AM2-Chem diagnosed stratospheric fraction of surface  $^7\text{Be}$  at NH mid-latitudes  
28 ( $\sim 25\text{--}30\%$ ) qualitatively agrees with the DH85 criterion (**Figure 11**). However, when it is  
29 included as part of the stratosphere, the corresponding fraction would dramatically increase to  
30  $\sim 45\%$  (not shown), reflecting the very coarse resolution ( $\sim 2\text{km}$ ) near the tropopause.

31 We previously assessed the cross-tropopause transport of  $^7\text{Be}$  in GEOS1-DAS and GEOS1-  
32 STRAT-DAS with the GEOS-Chem model (Liu et al., 2001). We extend the assessment to other



~~meteorological fields that drive GEOS-Chem, including GEOS3-DAS (2001), GEOS4-DAS (2004) and GEOS5-DAS (2004). GEOS4-DAS has been assessed earlier for cross-tropopause transport of  $^7\text{Be}$  with GMI-CTM but is included here for comparison purposes. In particular, GEOS5-DAS is a relatively newer version of the GEOS series of assimilated meteorological dataset available at NASA-GMAO. It is widely used in tropospheric chemistry modeling studies, for which characterizing cross-tropopause transport in GEOS5-DAS has important implications. **Figure 12** shows stratospheric fraction (%) of annual zonal mean tropospheric  $^7\text{Be}$  concentrations as a function of latitude and pressure as simulated by GEOS-Chem driven with GEOS3-DAS, GEOS4-DAS and GEOS5-DAS, respectively. Slower cross-tropopause transport is seen in GEOS3-DAS than in GEOS4-DAS and GEOS5-DAS. This may partly explain the low  $^7\text{Be}$  bias in the lower troposphere in a CTM driven with GEOS3-DAS (Allen et al., 2003). Overall, both GEOS4-DAS and GEOS5-DAS reasonably represent the impact of cross-tropopause transport on surface  $^7\text{Be}$  concentrations on the basis of the DH85 constraint. This suggests that models which utilize either of these fields could use the “Linoz” ozone scheme and expect satisfactory representation of the stratospheric influence on tropospheric ozone on a global scale. Nevertheless, GEOS5-DAS shows smaller STE influence in the middle troposphere than GEOS4-DAS and is more consistent with fvGCM (**Figure 12** vs. **Figure 6a**). Since fvGCM has more credible cross-tropopause transport than GEOS4-DAS (Section 5), this suggests that GEOS5-DAS improves the impact of cross-tropopause transport on the upper and middle troposphere relative to GEOS4-DAS.~~

## **67 Implications for cross-tropopause transport of ozone**

In this section we discuss the implications of different characteristics of cross-tropopause transport of  $^7\text{Be}$  for stratospheric influence on tropospheric ozone in different meteorological fields. At the time of this study, the GMI full-chemistry model can be driven with GEOS1-STRAT, fvGCM and GEOS4-DAS, but not GISS II' meteorological fields. This allows us to examine any potential relationship between the cross-tropopause transport of  $^7\text{Be}$  and ozone when these fields are used to drive the model.

Ozonesonde, surface and satellite observations provide useful constraints on the stratospheric contribution to tropospheric ozone (e.g., Rind et al., 2007; Lin et al., 2012). **Figure 13-11** shows comparisons of model tropospheric ozone profiles with annual mean ozonesonde observations for a range of latitudes (Considine et al., 2008). These results are typical of other stations at similar latitudes. The GMI/GEOS1-STRAT simulation produces excessive ozone throughout the

1 troposphere at all latitudes except in the tropics while the GMI/fvGCM and GMI/GEOS4-DAS  
2 simulations are generally in agreement with the observations (with slightly overpredicted ozone  
3 in the mid-latitude upper troposphere). The GEOS1-STRAT simulation has the largest greatest  
4 overestimate of O<sub>3</sub> in spring. We also compared model surface ozone concentrations with the  
5 Logan (1999) surface ozone dataset (not shown). Among the three GMI simulations, the  
6 GMI/GEOS1-STRAT simulation shows the largest errors in surface ozone concentrations during  
7 winter and spring when stratospheric contribution is at its peak. These are in line with the relative  
8 magnitudes of cross-tropopause transport efficiencies of <sup>7</sup>Be in the three meteorological fields  
9 (i.e., too fast STE in GEOS1-STRAT), discussed in previous sections. Indeed, the tropospheric  
10 version of the GMI/GEOS1-STRAT model with constrained STE flux of ozone using the Synoz  
11 approach (about 579 Tg/year) simulates ozonesonde observations of tropospheric ozone  
12 reasonably well (dotted line, **Figure 1311**).

13 **Figure 1412** shows GMI simulated annual zonal mean tropospheric ozone column (TOC), in  
14 Dobson Units, compared with observed climatologies from TOMS/SBUV (1979-2005; Fishman  
15 et al., 2003) and OMI/MLS (October 2004 - July 2008; Ziemke et al., 2006). The WMO  
16 definition of thermal tropopause is used to calculate the model TOC. While the GMI/fvGCM and  
17 GMI/GEOS4-DAS simulations are similar and overestimate TOC by up to ~20 DU, the  
18 GMI/GEOS1-STRAT simulation overestimates TOC by as much as ~40 DU. The excessive O<sub>3</sub>  
19 in the GMI/GEOS1-STRAT simulation with maxima at 30°N and 30°S suggests downward  
20 transport of ozone from the stratosphere is too fast. The tropospheric version of the  
21 GMI/GEOS1-STRAT model with constrained STE flux of ozone provides a much better  
22 simulation of global TOCs (red dashed line, **Figure 1412**), which are comparable to those from  
23 GMI/fvGCM and GMI/GEOS4-DAS simulations. However, model TOCs are still ~10-14DU  
24 larger than satellite observations in the subtropics and mid-latitudes. Previously, Ziemke et al.  
25 (2006) considered uncertainties in both model and observations and subjectively interpreted  
26 model-OMI/MLS TOC differences of 10 DU and higher as significant. As Stajner et al. (2008)  
27 noted, a low extratropical tropopause used by Ziemke et al. (2006) may have played an important  
28 role in the underestimation of OMI/MLS TOC. Yang et al. (2010) also found that their  
29 OMI/MLS potential vorticity mapped TOCs are smaller than ozonesonde TOCs by 5.9 DU with  
30 a standard deviation of the differences of 8.4 DU. On the other hand, the GMI/fvGCM  
31 simulation tends to overestimate ozone just below the tropopause at mid-latitudes (**Figure 1311**);  
32 these biases do not appear to be due to excessive stratospheric influence (Considine et al., 2008).  
33 Current global models also tend to overpredict surface ozone during summer and early fall over

the eastern U.S. and Japan (Fiore et al., 2009). Therefore the simulated TOCs are very likely biased high.

We further examine the relationship between the cross-tropopause transport of  $^7\text{Be}$  and ozone with the GEOS1-STRAT meteorological fields, in which case STE is known to be too fast.

**Figure 15a–13a** shows the latitudinal variations of annual zonal mean tropospheric  $^7\text{Be}$  column overestimate ( $\Delta^7\text{Be}$ ) and TOC overestimate ( $\Delta\text{TOC}$ ) in the GMI/GEOS1-STRAT simulation.  $\Delta^7\text{Be}$  is obtained by subtraction of the STE-flux-adjusted simulation (Section 2.4) from the standard simulation.  $\Delta\text{TOC}$  is obtained by subtracting the GMI tropospheric model simulation (with STE flux of ozone about 579 Tg/year) from the GMI full-chemistry model simulation.

**Figure 15b–13b** shows the correlation between the global distributions of  $\Delta^7\text{Be}$  and  $\Delta\text{TOC}$ . The lines of best fit are calculated using the reduced-major-axis (RMA) method (Hirsch and Gilroy, 1984). Standard errors for the intercept and the slope are computed as described by Miller and Kahn (1962). Overall, the location of overestimated ozone follows that of overestimated  $^7\text{Be}$ , with both maxima near  $30^\circ\text{N}$  and  $30^\circ\text{S}$ . The strong correlation between  $\Delta^7\text{Be}$  and  $\Delta\text{TOC}$  implies that  $^7\text{Be}$  is a good indicator of cross-tropopause transport of ozone. These support our conclusion that  $^7\text{Be}$  is a useful utility for assessing cross-tropopause transport of ozone in global models.

## **8–7 Summary and conclusions**

We have assessed the ability of the Global Modeling Initiative (GMI) chemical transport model (CTM) using different meteorological data sets to simulate the atmospheric distributions of  $^7\text{Be}$ , a natural aerosol tracer originating from the upper troposphere/lower stratosphere and removed from the troposphere primarily by wet deposition. The model was driven by four meteorological data sets (GEOS1-STRAT, GISS\_II', fvGCM, GEOS4-DAS) which feature significantly different cross-tropopause transport characteristics. The GMI modeling framework was configured such that the variability between the simulations mainly reflects the use of different meteorological data. Our goal was to assess the utility of  $^7\text{Be}$  as a tracer of cross-tropopause transport in global models and develop a methodology to exploit such a utility. We have also discussed the implications of excessive cross-tropopause transport as revealed by  $^7\text{Be}$  simulations for the modeling of tropospheric ozone.

We evaluated the four simulations of  $^7\text{Be}$  with RANDAB, a unique database of upper atmosphere radionuclide climatological observations compiled by the DOE (now DHS) Environmental Measurement Laboratory, as well as long-term measurements at the surface. Model simulations capture the UT/LS observations with respect to latitudes. The GMI/GEOS1-

1 STRAT simulation shows the lowest  $^7\text{Be}$  concentrations among the four simulations in the lower  
2 stratosphere, and underestimates the observations. This reflects the well-known highly  
3 overestimated cross-tropopause transport in GEOS1-STRAT DAS. At the surface, GMI/GISS II'  
4 reproduces the observed latitudinal trends of  $^7\text{Be}$  concentrations, but shows too high  
5 concentrations at high latitudes. The GMI/fvGCM simulated  $^7\text{Be}$  deposition fluxes are the closest  
6 to the observations, while the GMI/GEOS1-STRAT overestimates the observed  $^7\text{Be}$  deposition  
7 fluxes at subtropical latitudes by up to a factor of 2.5 (30°N) and the GMI/GISS simulations at  
8 high latitudes (45-60°N) are too high by a factor of 2. We were able to show that the observed  
9  $^7\text{Be}$  deposition fluxes offer a strong constraint on stratosphere-to-troposphere transport in global  
10 models.

11 We examined the observational constraint from Dutkiewicz and Husain (1985) (DH85) on  
12 the stratospheric contribution to tropospheric  $^7\text{Be}$  using the GMI modeling framework. DH85  
13 analyzed the observed  $^7\text{Be}/^{90}\text{Sr}$  ratio, which suggests that 23-27% of the  $^7\text{Be}$  in surface air at  
14 northern mid-latitudes is of stratospheric origin. This constraint offers a sensitive test of cross-  
15 tropopause transport in global models. Comparison of the fraction of surface air of stratospheric  
16 origin estimated from the  $^7\text{Be}$  simulations with the DH85 constraint indicates excessive cross-  
17 tropopause transport at mid-latitudes with the GEOS1-STRAT meteorological fields and at high  
18 latitudes with the GISS II' fields. Interestingly, these simulations also overestimate observed  $^7\text{Be}$   
19 deposition fluxes at middle and high latitudes, respectively. With a correction to cross-  
20 tropopause flux, the model simulates better surface  $^7\text{Be}$  concentrations and total deposition  
21 fluxes. By contrast, the fvGCM meteorological data yield the most reasonable cross-tropopause  
22 transport of  $^7\text{Be}$  according to the DH85 constraint, consistent with the fact that the GMI/fvGCM  
23 simulated  $^7\text{Be}$  deposition fluxes are closest to the observations. These results illustrate that the  
24 GMI framework is very useful for characterizing and helping reduce uncertainties in the  
25 processes such as cross-tropopause transport in the meteorological fields that are used to drive  
26 chemical transport models. Note that since wet deposition removes both the stratospheric and  
27 tropospheric components of  $^7\text{Be}$  nondiscriminatively, the model diagnosed fraction of  $^7\text{Be}$  of  
28 stratospheric origin does not significantly depend on the rate of wet removal.

29 The model diagnosed stratospheric fraction of  $^7\text{Be}$  in surface air is sensitive to the diagnosed  
30 location of tropopause, in particular when the model vertical resolution is relatively coarse (>1-  
31 1.5km) near the tropopause region. This suggests that stratospheric fraction of  $^7\text{Be}$  is a more  
32 useful diagnostic when the model has sufficient vertical resolution (<1-1.5km) so that the  
33 tropopause can be well defined. We used the WMO definition of thermal tropopause and include

1 the diagnosed tropopause model layer as part of the troposphere (versus the stratosphere). As  
2 such our assessment of cross-tropopause transport of  $^7\text{Be}$  in the four meteorological data sets in  
3 the GMI CTM is consistent with previous modeling studies of stratospheric influence on  
4 tropospheric ozone.

5 ~~We further applied the DH85 constraint to assess cross-tropopause transport of  $^7\text{Be}$  in other~~  
6 ~~meteorological data sets or models, including GFDL AM2 GCM (via online simulation),~~  
7 ~~GEOS3-DAS and GEOS5-DAS (via offline GEOS-Chem model simulation). The diagnosed~~  
8 ~~stratospheric fraction of surface  $^7\text{Be}$  at NH mid-latitudes in AM2 qualitatively agrees with the~~  
9 ~~DH85 constraint. However, this diagnostic has a large uncertainty due to the coarse resolution~~  
10 ~~near the tropopause region in AM2. Slower cross-tropopause transport is seen in GEOS3-DAS~~  
11 ~~than in GEOS4-DAS and GEOS5-DAS; the latter two meteorological fields represent the impact~~  
12 ~~of cross-tropopause transport on surface  $^7\text{Be}$  concentrations reasonably well. One of the~~  
13 ~~implications is that it would be appropriate to implement “Linoz” ozone (McLinden et al., 2000)~~  
14 ~~in a chemical transport model driven with GEOS4-DAS or GEOS5-DAS. On the other hand,~~  
15 ~~similar to fvGCM, GEOS5-DAS appears to show a smaller impact of cross-tropopause transport~~  
16 ~~on the upper and middle troposphere, which is improved relative to GEOS4-DAS.~~

17 Incorrect cross-tropopause transport of  $^7\text{Be}$  implies misrepresented downward influx of  
18 stratospheric ozone to the troposphere in a model. We demonstrated this by examining the  
19 relationship between the cross-tropopause transport of  $^7\text{Be}$  and ozone as simulated by GMI CTM  
20 driven with GEOS1-STRAT, fvGCM and GEOS4-DAS meteorological fields. We found that  
21 excessive cross-tropopause transport of  $^7\text{Be}$  corresponds to overestimated stratospheric  
22 contribution to tropospheric ozone, as constrained by ozonesonde, surface and satellite  
23 observations.

24 In summary, the  $^7\text{Be}$  simulation, which is computationally cheap and technically simple, in  
25 combination with the DH85  $^7\text{Be}$  observational constraint and observed  $^7\text{Be}$  deposition fluxes  
26 may be used routinely to assess cross-tropopause transport in global models. We recommend  
27 separate transport of the  $^7\text{Be}$  produced in the stratosphere ( $^7\text{Be}$ -strat) to evaluate the ratio of  $^7\text{Be}$ -  
28 strat to total  $^7\text{Be}$  (i.e., beryllium-7 produced in both the stratosphere and the troposphere) in  
29 surface air against the DH85 constraint. This can serve as a first-order assessment of cross-  
30 tropopause transport in the meteorological fields ~~and therefore help determine whether either~~  
31 ~~“Synoz” or “Linoz” ozone should be used for the stratosphere in the studies that focus on the~~  
32 ~~troposphere. With improved estimates of  $^7\text{Be}$  production rates as well as their year-to-year~~  
33 ~~variations, model multi-year  $^7\text{Be}$  simulations together with long-term observations would~~

1 provide useful constraints on the interannual variability of STE. While this study uses  $^7\text{Be}$  alone,  
2 future modeling work will include using  $^{10}\text{Be}/^7\text{Be}$ , a more sensitive indicator of STE (Rehfeld  
3 and Heimann, 1995; Koch and Rind, 1998; Jordan et al., 2003), ~~within the GMI modeling~~  
4 ~~framework.~~

## 6 **Acknowledgments**

7 This work was supported by the NASA Modeling, Analysis and Prediction (MAP) program,  
8 the Atmospheric Composition Modeling and Analysis Program (ACMAP), and the Atmospheric  
9 Composition Campaign Data Analysis and Modeling (ACCDAM) program, ~~and by NOAA~~  
10 ~~Geophysical Fluid and Dynamics Laboratory (GFDL).~~ We thank Bryan Duncan for his  
11 contribution to the GMI model development. The GMI core team at NASA GSFC is  
12 acknowledged for programming support. NASA Center for Computational Sciences (NCCS) ~~and~~  
13 ~~GFDL~~ provided supercomputing resources. The GEOS-Chem model is managed by the  
14 Atmospheric Chemistry Modeling Group at Harvard University with support from ACPMAP and  
15 MAP.

## References

- Adler, R. F.: The Version 2 Global Precipitation Climatology Project (GPCP) monthly precipitation analysis (1979-Present), *J. Hydrometeorol.*, 4, 1147-1167, 2003.
- Allen, D. J., Dibb, J. E., Ridley, B., Pickering, K. E., and Talbot, R. W.: An estimate of the stratospheric contribution to springtime tropospheric ozone maxima using TOPSE measurements and beryllium-7 simulations, *J. Geophys. Res.*, 108(D4), 8355, doi:10.1029/2001JD001428, 2003.
- Bey, I., Jacob, D. J., Yantosca, R. M., Logan, J. A., Field, B., Fiore, A. M., Li, Q., Liu, H., Mickley, L. J., and Schultz, M.: Global modeling of tropospheric chemistry with assimilated meteorology: Model description and evaluation, *J. Geophys. Res.*, 106, 23,073-23,096, 2001.
- Brost, R. A., Feichter, J., and Heimann, M.: Three-dimensional simulation of  $^7\text{Be}$  in a global climate model, *J. Geophys. Res.*, 96(D12), 22,423-22,445, 1991.
- Collins, W. J., Derwent, R. G., Garnier, B., Johnson, C. E., and Sanderson, M. G., and Stevenson, D. S.: Effect of stratosphere-troposphere exchange on the future tropospheric ozone trend, *J. Geophys. Res.*, 108(D12), 8528, doi:10.1029/2002JD002617, 2003.
- Considine, D. B., Bergmann, D. J., and Liu, H.: Sensitivity of Global Modeling Initiative chemistry and transport model simulations of radon-222 and lead-210 to input meteorological data, *Atmos. Chem. Phys.*, 5, 3389-3406, 2005.
- Considine, D. B., Logan, J. A., and Olsen, M. A.: Evaluation of near-tropopause ozone distributions in the Global Modeling Initiative combined stratosphere/troposphere model with ozonesonde data, *Atmos. Chem. Phys.*, 8, 2365-2385, 2008.
- Cristofanelli, P., Bonasoni, P., Collins, W., Feichter, J., Forster, C., James, P., Kentarchos, A., Kubik, P. W., Land, C., Meloen, J., Roelofs, G. J., Siegmund, P., Sprenger, M., Schnabel, C., Stohl, A., Tobler, L., Tositti, L., Trickl, T., and Zanis, P.: Stratosphere-to-troposphere transport: A model and method evaluation, *J. Geophys. Res.*, 108(D12), 8525, doi:10.1029/2002JD002600, 2003.
- Dibb, J. E., Talbot, R. W., and Gregory, G. L.: Beryllium 7 and lead 210 in the western hemisphere Arctic atmosphere: Observations from three recent aircraft-based sampling programs, *J. Geophys. Res.*, 97(D15), 16,709–16,715, 1992.



- 1 Dobb, J. E., Meeker, L. D., Finkel, R. C., Southon, J. R., Caffee, M. W., and Barrie, L. A.:  
2 Estimation of stratospheric input to the Arctic troposphere:  $^7\text{Be}$  and  $^{10}\text{Be}$  in aerosols at Alert,  
3 Canada, *J. Geophys. Res.*, 99(D6), 12,855–12,864, 1994.
- 4 Dobb, J. E., Talbot, R. W., Scheuer, E., Seid, G., DeBell, L., Lefer, B., and Ridley, B.:  
5 Stratospheric influence on the northern North American free troposphere during TOPSE:  $^7\text{Be}$   
6 as a stratospheric tracer, *J. Geophys. Res.*, 108(D4), 8363, doi:10.1029/2001JD001347, 2003.
- 7 Dobb, J. E.: Vertical mixing above Summit, Greenland: Insights into seasonal and high frequency  
8 variability from the radionuclide tracers Be-7 and Pb-210, *Atmos. Environ.*, 41(24), 5020-  
9 5030, 2007.
- 10 Douglass, A. R., Prather, M. J., Hall, T. M., Strahan, S. E., Rasch, P. J., Sparling, L. C., Coy, L.,  
11 and Rodriguez, J. M.: Choosing meteorological input for the Global Modeling Initiative  
12 assessment of high-speed aircraft, *J. Geophys. Res.*, 104(D22), 27,545-27,564, 1999.
- 13 Douglass, A. R., Schoeberl, M. R., Rood, R. B., and Pawson, S.: Evaluation of transport in the  
14 lower tropical stratosphere in a global chemistry and transport model, *J. Geophys. Res.*,  
15 108(D9), 4259, doi:10.1029/2002JD002696, 2003.
- 16 Douglass, A. R., Stolarski, R. S., Strahan, S. E., and Connell, P. S.: Radicals and reservoirs in the  
17 GMI chemistry and transport model: Comparison to measurements, *J. Geophys. Res.*, 109,  
18 D16302, doi:10.1029/2004JD004632, 2004.
- 19 Douglass, A. R., Stolarski, R. S., Schoeberl, M. R., Jackman, C. H., Gupta, M. L., Newman, P.  
20 A., Nielsen, J. E., and Fleming, E. L.: Relationship of loss, mean age of air and  
21 the distribution of CFCs to stratospheric circulation and implications for atmospheric  
22 lifetimes, *J. Geophys. Res.*, 113, D14309, doi:10.1029/2007JD009575, 2008.
- 23 Duncan, B. N., Strahan, S. E., and Yoshida, Y.: Model study of the cross-tropopause transport of  
24 biomass burning pollution, *Atmos. Chem. Phys.*, 7, 3713-3736, 2007.
- 25 Duncan, B., et al.: The influence of European pollution on ozone in the Near East and northern  
26 Africa, *Atmos. Chem. Phys.*, 8, 2267-2283, 2008.
- 27 Dutkiewicz, V. A., and Husain, L.: Stratospheric and tropospheric components of  $^7\text{Be}$  in surface  
28 air, *J. Geophys. Res.*, 90, 5783-5788, 1985.
- 29 Feely, H. W., Larsen, R. J., and Sanderson, C. G.: Factors that cause seasonal variations in  
30 beryllium-7 concentrations in surface air, *J. Environ. Radioactivity*, 9, 223-249, 1989.



- Field, C. V., Schmidt, G. A., Koch, D., and Salyk, C.: Modeling production and climate-related impacts on  $^{10}\text{Be}$  concentration in ice cores, *J. Geophys. Res.*, 111, D15107, doi:10.1029/2005JD006410, 2006.
- ~~Fiore, A. M., Dentener, F. J., wild, O., Cuvelier, C., Schultz, M. G., Hess, P., Textor, C., Schulz, M., Doherty, R. M., Horowitz, L. W., MacKenzie, I. A., Sanderson, M. G., Shindell, D. T., Stevenson, D. S., Szopa, S., Van Dingenen, R., Zeng, G., Atherton, C., Bergmann, D., Bey, I., Carmichael, G., Collins, W. J., Duncan, B. N., Faluvegi, G., Folberth, G., Gauss, M., Gong, S., Hauglustaine, D., Holloway, T., Isaksen, I. S. A., Jacob, D. J., Jonson, J. E., Kaminski, J. W., Keating, T. J., Lupu, A., Marmer, E., Montanaro, V., Park, R. J., Pitari, G., Pringle, K. J., Pyle, J. A., Schroeder, S., Vivanco, M. G., Wind, P., Wojcik, G., Wu, S., and Zuber, A.~~ ~~Fiore, A. M., et al.~~: Multimodel estimates of intercontinental source-receptor relationships for ozone pollution, *J. Geophys. Res.*, 114, D04301, doi:10.1029/2008JD010816, 2009.
- Fishman, J., Wozniak, A. E., and Creilson, J. K.: Global distribution of tropospheric ozone from satellite measurements using the empirically corrected tropospheric ozone residual technique: Identification of the regional aspects of air pollution, *Atmos. Chem. Phys.*, 3, 893-907, 2003.
- ~~GFDL GAMDT: The new GFDL global atmosphere and land model AM2 LM2: Evaluation with prescribed SST simulations, *J. Climate*, 17, 4,641-4,673, 2004.~~
- Graustein, W. C., and Turekian, K. K.:  $^7\text{Be}$  and  $^{210}\text{Pb}$  indicate an upper troposphere source for elevated ozone in the summertime subtropical free troposphere of the eastern North Atlantic, *Geophys. Res. Lett.*, 23, 539-542, 1996.
- Heikkila, U., Beer, J., and Alfimov, V.: Beryllium-10 and beryllium-7 in precipitation in Dubendorf (440 m) and at Jungfraujoch (3580 m), Switzerland (1998-2005), *J. Geophys. Res.*, 113, D11104, doi:10.1029/2007JD009160, 2008a.
- Heikkila, U., Beer, J., and Feichter, J.: Modeling cosmogenic radionuclides  $^{10}\text{Be}$  and  $^7\text{Be}$  during the Maunder Minimum using the ECHAM5-HAM general circulation model, *Atmos. Chem. Phys.*, 8, 2797-2809, 2008b.
- Helmig, D., Oltmans, S. J., Morse, T. O., and Dibb, J. E.: What is causing high ozone at Summit, Greenland? *Atmos. Environ.*, 41, 5031-5043, 2007.

- 1 Hirsch, R. M., and Gilroy, E. J.: Methods of fitting a straight line to data: Examples in water  
2 resources, Water Res. Bull., 20, 705-711, 1984.
- 3 Holton, J. R., Haynes, P. H., McIntyre, M. E., Douglass, A. R., Rood, R. B., and Pfister, L.:  
4 Stratosphere-Troposphere Exchange, Rev. Geophys., 33(4), 403-439, 1995.
- 5 ~~Horowitz, L. W.: A global simulation of tropospheric ozone and related tracers: Description and~~  
6 ~~evaluation of MOZART, version 2, J. Geophys. Res., 108(D24), 4784,~~  
7 ~~doi:10.1029/2002JD002853, 2003.~~
- 8 Hsu, J., Prather, M. J., and Wild, O.: Diagnosing the stratosphere-to-troposphere flux of ozone in  
9 a chemistry transport model, J. Geophys. Res., 110, D19305, doi:10.1029/2005JD006045,  
10 2005.
- 11 Hsu, J., and Prather, M. J.: Stratospheric variability and tropospheric ozone, J. Geophys. Res.,  
12 114, D06102, doi:10.1029/2008JD010942, 2009.
- 13 Husain, L., Coffey, P. E., Meyers, R. E., and Cederwall, R. T.: Ozone transport from stratosphere  
14 to troposphere, Geophys. Res. Lett., 4, 363-365, 1977.
- 15 Johnson, W. B., and Viezee, W.: Stratospheric ozone in the lower troposphere – I. Presentation  
16 and interpretation of aircraft measurements, Atmos. Environ., 15, 1309-1323, 1981.
- 17 Jordan, C. E., Dibb, J. E., and Finkel, R. C.:  $^{10}\text{Be}/^7\text{Be}$  tracer of atmospheric transport and  
18 stratosphere-troposphere exchange, J. Geophys. Res., 108(D8), 4234,  
19 doi:10.1029/2002JD002395, 2003.
- 20 Koch, D. M., Jacob, D. J., and Graustein, W. C.: Vertical transport of tropospheric aerosols as  
21 indicated by  $^7\text{Be}$  and  $^{210}\text{Pb}$  in a chemical tracer model, J. Geophys. Res., 101, 18,651-18,666,  
22 1996.
- 23 Koch, D. M., and Rind, D.: Beryllium 10/beryllium 7 as a tracer of stratospheric transport, J.  
24 Geophys. Res., 103(D4), 3907-3917, 1998.
- 25 Koch, D., Schmidt, G. A., and Field, C. V.: Sulfur, sea salt, and radionuclide aerosols in GISS  
26 ModelE, J. Geophys. Res., 111, D06206, doi:10.1029/2004JD005550, 2006.
- 27 Kritz, M. A., Rosner, S. W., Danielsen, E. F., and Selkirk, S. B.: Air mass origins and  
28 troposphere-to-stratosphere exchanges associated with mid-latitude cyclogenesis and  
29 tropopause folding inferred from  $^7\text{Be}$  measurements, J. Geophys. Res., 96, 17,405-17,414,  
30 1991.

- Lal, D., and Peters, B.: Cosmic ray produced radioactivity on the Earth, in Handbuch der Physik, 46/2, edited by K. Sitte, pp.551-612, Springer-Verlag, New York, 1967.
- [Langford, A. O., Senff, C. J., Alvarez II, R. J., Brioude, J., Cooper, O. R., Holloway, J. S., Lin, M. Y., Marchbanks, R. D., Pierce, R. B., Sandberg, S. P., Weickmann, A. M., Williams, E. J.: An overview of the 2013 Las Vegas Ozone Study \(LVOS\): Impact of stratospheric intrusions and long-range transport on surface air quality. Atmos. Environ. doi:10.1016/j.atmosenv.2014.08.040, 2014 C8629 ACPD 15, C8628–C8630, 2015](#)
- Li, Q., Jacob, D. J., Fairlie, T. D., Liu, H., Martin, R. V., and Yantosca, R. M.: Stratospheric versus pollution influences on ozone at Bermuda: Reconciling past analyses, J. Geophys. Res., 107(D22), 4611, doi:10.1029/2002JD002138, 2002.
- Liang, Q., Douglass, A. R., Duncan, B. N., Stolarski, R. S., and Witte, J. C.: The governing processes and timescales of stratosphere-to-troposphere transport and its contribution to ozone in the Arctic troposphere, Atmos. Chem. Phys., 9, 3011-3025, 2009.
- [Lin, S. J. and Rood, R. B.: Multidimensional flux-form semi-Lagrangian transport schemes, Mon. Weather Rev., 124\(9\), 2046-2070, 1996.](#)
- Lin, M., A. M. Fiore, O. R. Cooper, L. W. Horowitz, A. O. Langford, H. Levy II, B. J. Johnson, V. Naik, S. J. Oltmans, and C. J. Senff (2012), Springtime high surface ozone events over the western United States: Quantifying the role of stratospheric intrusions, J. Geophys. Res., 117, D00V22, doi:10.1029/2012JD018151.
- [Lin, M., Fiore, A. M., Horowitz, L. W., Langford, A. O., Oltmans, S. J., Tarasick, D., and Rieder, H. E.: Climate variability modulates western U.S. ozone air quality in spring via deep stratospheric intrusions, Nature Communications, 6 \(7105\), doi: 10.1038/ncomms8105, 2015.](#)
- Liu, H., Jacob, D. J., Bey, I., and Yantosca, R. M.: Constraints from  $^{210}\text{Pb}$  and  $^7\text{Be}$  on wet deposition and transport in a global three-dimensional chemical tracer model driven by assimilated meteorological fields, J. Geophys. Res., 106, 12,109-12,128, 2001.
- Liu, H., Jacob, D. J., Dibb, J. E., Fiore, A. M., and Yantosca, R. M.: Constraints on the sources of tropospheric ozone from  $^{210}\text{Pb}$ - $^7\text{Be}$ - $\text{O}_3$  correlations, J. Geophys. Res., 109, D07306, doi:10.1029/2003JD003988, 2004.

- 1 Liu, X., Penner, J. E., Das, B., Bergmann, D., Rodriguez, J. M., Strahan, S., M. Wang, M., and  
2 Y. Feng, Y.: Uncertainties in global aerosol simulations: Assessment using three  
3 meteorological data sets, *J. Geophys. Res.*, 112, D11212, doi:10.1029/2006JD008216, 2007.
- 4 Logan, J. A.: An analysis of ozonesonde data for the troposphere: Recommendations for testing  
5 3-D models, and development of a gridded climatology for tropospheric ozone, *J. Geophys.*  
6 *Res.*, 104, 16,115-16,149, 1999.
- 7 Masarik, J., and Beer, J.: Simulation of particle fluxes and cosmogenic nuclide production in the  
8 Earth's atmosphere, *J. Geophys. Res.*, 104, 12,099-12,111, 1999.
- 9 Masarik, J., and Reedy, R. C.: Terrestrialcosmogenic-nuclide production systematic calculated  
10 from numerical simulations, *Earth Planet. Sci. Lett.* 136, 381–395, 1995.
- 11 McLinden, C. A., Olsen, S. C., Hannegan, B., Wild, O., and M. J. Prather: Stratospheric ozone in  
12 3-D models: A simple chemistry and the cross-tropopause flux, *J. Geophys. Res.*, 105,  
13 14,653-14,665, 2000.
- 14 Miller, R. L., and J.S. Kahn, J. S.: Statistical analysis in the geological sciences, p204-210, John  
15 Wiley and Sons, New York, New York, 1962.
- 16 Murphy, D. M., and Fahey, D. W.: An estimate of the flux of stratospheric reactive nitrogen and  
17 ozone into the troposphere, *J. Geophys. Res.*, 99, 5,325-5,332, 1994.
- 18 O'Brien, K., De La Zerda Lerner, A., Shea, M. A., and Smart, D. F.: The production of  
19 cosmogenic isotopes in the Earth's atmosphere and their inventories, in *The Sun in Time*,  
20 pp.317-342, Univ. of Ariz. Press, Tucson, 1991.
- 21 Olsen, M. A., Schoeberl, M. R., and Douglass, A. R.: Stratosphere-troposphere exchange of mass  
22 and ozone, *J. Geophys. Res.*, 109, D24114, doi:10.1029/2004JD005186, 2004.
- 23 Prospero, J. M., Schmitt, R., Curvas, E., Savoie, D. L., Graustein, W. C., Turekian, K. K., Volz-  
24 Thomas, A., Diaz, A., Oltmans, S. J., and Levy II, H.: Temporal variability of summer-time  
25 ozone and aerosols in the free troposphere over the eastern North Atlantic, *Geophys. Res.*  
26 *Lett.*, 22, 2,925-2,928, 1995.
- 27 Raisbeck, G. M., Yiou, F., Fruneau, M., Loiseaux, J. M., Lieuvin, M., and Ravel, J. C.:  
28 Cosmogenic Be-10/Be-7 as a probe for atmospheric transport processes, *Geophys. Res. Lett.*,  
29 8, 1015-1018, 1981.

- 1 Rehfeld, S. and Heimann, M.: Three dimensional atmospheric transport simulation of the  
2 radioactive tracers  $^{210}\text{Pb}$ ,  $^7\text{Be}$ ,  $^{10}\text{Be}$ , and  $^{90}\text{Sr}$ , J. Geophys. Res., 100(D12), 26,141-26,161,  
3 1995.
- 4 [Riese, M., Ploeger, F., Rap, A., Vogel, B., Konopka, P., Dameris, M., and Forster, P.: Impact of](#)  
5 [uncertainties in atmospheric mixing on simulated UTLS composition and related radiative](#)  
6 [effects, J. Geophys. Res., 117, D16305, doi:10.1029/2012JD017751, 2012.](#)
- 7 Rind, D., Lerner, J., Jonas, J., and McLinden, C.: Effects of resolution and model physics on  
8 tracer transports in the NASA Goddard Institute for Space Studies general circulation  
9 models, J. Geophys. Res., 112, D09315, doi:10.1029/2006JD007476, 2007.
- 10 [Rotman, D. A., Tannahill, J. R., Kinnison, D. E., Connell, P. S., Bergmann, D., Proctor, D.,](#)  
11 [Rodriguez, J. M., Lin, S. J., Rood, R. B., Prather, M. J., Rasch, P. J., Considine, D. B.,](#)  
12 [Ramaroson, R., and Kawa, S. R.:](#) Global Modeling Initiative assessment model: Model  
13 description, integration, and testing of the transport shell, J. Geophys. Res., 106, 1669-1691,  
14 2001.
- 15 Sanak, J., Lambert, G., and Ardouin, B.: Measurements of stratosphere-troposphere exchange in  
16 Antarctica by using short-lived cosmonuclides, Tellus, Ser. B, 37, 109-115, 1985.
- 17 Schoeberl, M. R., Douglass, A. R., Zhu, Z., and Pawson, S.: A comparison of the lower  
18 stratospheric age spectra derived from a general circulation model and two data assimilation  
19 systems, J. Geophys. Res., 108(D3), 4113, doi:10.1029/2002JD002652, 2003.
- 20 Schoeberl, M. R.: Extratropical stratosphere-troposphere mass exchange, J. Geophys. Res., 109,  
21 D13303, doi:10.1029/2004JD004525, 2004.
- 22 Shindell, D. T., Faluvegi, G., and Bell, N.: Preindustrial-to-present-day radiative forcing by  
23 tropospheric ozone from improved simulations with the GISS chemistry-climate GCM,  
24 Atmos. Chem. Phys., 3, 1675-1702, 2003.
- 25 [Škerlak, B., Sprenger, M., and Wernli, H.: A global climatology of stratosphere–troposphere](#)  
26 [exchange using the ERA-Interim data set from 1979 to 2011, Atmos. Chem. Phys., 14, 913-](#)  
27 [937, doi:10.5194/acp-14-913-2014, 2014.](#)
- 28 [Stajner, I., Wargan, K., Pawson, S., Hayashi, H., Chang, L.-P., Hudman, R. C., Froidevaux, L.,](#)  
29 [Livesey, N., Levelt, P. F., Thompson, A. M., Tarasick, D. W., Stubi, R., Andersen, S. B.,](#)  
30 [Yela, M., Konig-Langlo, G., Schmidlin, F. J., and Witte, J. C.:](#) Assimilated ozone from EOS-

Aura: Evaluation of the tropopause region and tropospheric columns, J. Geophys. Res., 113, D16S32, doi:10.1029/2007JD008863, 2008.

Stevenson, D. S., Dentener, F. J., Schultz, M. G., Ellingsen, K., van Noije, T. P. C., Wild, O., Zeng, G., Amann, M., Atherton, C. S., Bell, N., Bergmann, D. J., Bey, I., Butler, T., Cofala, J., Collins, W. J., Derwent, R. G., Doherty, R. M., Drevet, J., Eskes, H. J., Fiore, A. M., Gauss, M., Hauglustaine, D. A., Horowitz, L. W., Isaksen, I. S. A., Krol, M. C., Lamarque, J. -F., Lawrence, M. G., Montanaro, V., Müller, J. -F., Pitari, G., Prather, M. J., Pyle, J. A., Rast, S., Rodriguez, J. M., Sanderson, M. G., Savage, N. H., Shindell, D. T., Strahan, S. E., Sudo, K., and Szopa, S.: Multimodel ensemble simulations of present-day and near-future tropospheric ozone, J. Geophys. Res., 111, D08301, doi:10.1029/2005JD006338, 2006.

Stohl, A., Bonasoni, P., Cristofanelli, P., Collins, W., Feichter, J., Frank, A., Forster, C., Gerasopoulos, E., Gäggeler, H., James, P., Kentarchos, T., Kromp-Kolb, H., Krüger, B., Land, C., Meloen, J., Papayannis, A., Priller, A., Seibert, P., Sprenger, M., Roelofs, G. J., Scheel, H. E., Schnabel, C., Siegmund, P., Tobler, L., Trickl, T., Wernli, H., Wirth, V., Zanis, P., and Zerefos, C.: Stratosphere-troposphere exchange: A review, and what we have learnt from STACCATO, J. Geophys. Res., 108(D12), 8516, doi:10.1029/2002JD002490, 2003.

Strahan, S. E., and Douglass, A. R.: Evaluating the credibility of transport processes in simulations of ozone recovery using the Global Modeling Initiative three-dimensional model, J. Geophys. Res., 109, D05110, doi:10.1029/2003JD004238, 2004.

Strahan, S. E., Duncan, B. N., and Hoor, P.: Observationally-derived diagnostics of transport in the lowermost stratosphere and their application to the GMI chemistry transport model, Atmos. Chem. Phys., 7, 2435-2445, 2007.

Strahan, S. E., Schoeberl, M. R., and Steenrod, S. D.: The impact of tropical recirculation on polar composition, Atmos. Chem. Phys., 9, 2471-2480, 2009.

Terao, Y., Logan, J. A., Douglass, A. R., and R.S. Stolarski, R. S.: Contribution of stratospheric ozone to the interannual variability of tropospheric ozone in the northern extratropics, J. Geophys. Res., 113, D18309, doi:10.1029/2008JD009854, 2008.

Thompson, A. M., Witte, J. C., McPeters, R. D., Oltmans, S. J., Schmidlin, F. J., Logan, J. A., Fujiwara, M., Kirchhoff, V. W. J. H., Posny, F., Coetzee, G. J. R., and Hoegger, B., Kawakami, S., Ogawa, T., Johnson, B. J., Vömel, H., and Labow, G.: Southern Hemisphere

- 1 Additional Ozonesondes (SHADOZ) 1998–2000 tropical ozone climatology – 1. Comparison  
2 with Total Ozone Mapping Spectrometer (TOMS) and groundbased measurements, J.  
3 Geophys. Res., 108(D2), 8238, doi:10.1029/2001JD000967, 2003.
- 4 Tsutsumi, Y., Igarashi, Y., Zaizen, Y., and Makino, Y.: Case studies of tropospheric ozone  
5 events observed at the summit of Mount Fuji, J. Geophys. Res., 103, 16,935-16,951, 1998.
- 6 Usoskin, I. G., and Kovaltsov, G. A.: Production of cosmogenic  $^7\text{Be}$  isotope in the atmosphere:  
7 Full 3-D modeling, J. Geophys. Res., 113, D12107, doi:10.1029/2007JD009725, 2008.
- 8 Viezee, W., and Singh, H. B.: The distribution of beryllium-7 in the troposphere: Implications on  
9 stratosphere/tropospheric air exchange, Geophys. Res. Lett., 7, 805-808, 1980.
- 10 Yang, Q., Cunnold, D. M., Choi, Y., Wang, Y., Nam, J., Wang, H. -J., Froidevaux, L.,  
11 Thompson, A. M., and Bhartia, P. K.: A study of tropospheric ozone column enhancements  
12 over North America using satellite data and a global chemical transport model, J. Geophys.  
13 Res., 115, D08302, doi:10.1029/2009JD012616, 2010.
- 14 Young, P. J., Archibald, A. T., Bowman, K. W., Lamarque, J.-F., Naik, V., Stevenson, D. S.,  
15 Tilmes, S., Voulgarakis, A., Wild, O., Bergmann, D., Cameron-Smith, P., Cionni, I., Collins,  
16 W. J., Dalsøren, S. B., Doherty, R. M., Eyring, V., Faluvegi, G., Horowitz, L. W., Josse, B.,  
17 Lee, Y. H., MacKenzie, I. A., Nagashima, T., Plummer, D. A., Righi, M., Rumbold, S. T.,  
18 Skeie, R. B., Shindell, D. T., Strode, S. A., Sudo, K., Szopa, S., and Zeng, G.: Pre-industrial  
19 to end 21st century projections of tropospheric ozone from the Atmospheric Chemistry and  
20 Climate Model Intercomparison Project (ACCMIP), Atmos. Chem. Phys., 13, 2063-2090,  
21 doi:10.5194/acp-13-2063-2013, 2013.
- 22 Zanis, P., Gerasopoulos, E., Priller, A., Schnabel, C., Stohl, A., Zerefos, C., Gäggeler, H. W.,  
23 Tobler, L., Kubik, P. W., Kanter, H. J., Scheel, H. E., Luterbacher, J., and Berger, M.: An  
24 estimate of the impact of stratosphere-to-troposphere transport (STT) on the lower free  
25 tropospheric ozone over the Alps using  $^{10}\text{Be}$  and  $^7\text{Be}$  measurements, J. Geophys. Res.,  
26 108(D12), 8520, doi:10.1029/2002JD002604, 2003.
- 27 Ziemke, J. R., Chandra, S., Duncan, B. N., Froidevaux, L., Bhartia, P. K., Levelt, P. F., and  
28 Waters, J. W.: Tropospheric ozone determined from Aura OMI and MLS: Evaluation of  
29 measurements and comparison with the Global Modeling Initiative's Chemical Transport  
30 Model, J. Geophys. Res., 111, D19303, doi:10.1029/2006JD007089, 2006.

1  
2  
3  
4  
  
  
  
5  
6  
7  
8

Table 1. Acronyms of the models and driving meteorological data sets

Model / Data Set	Acronym
GMI CTM	Global Modeling Initiative Chemical Transport Model
GEOS1-STRAT DAS	Goddard Earth Observing System Data Assimilation System – version 1 in support of the Stratospheric Tracers of Atmospheric Transport mission
GISS II’ GCM	Goddard Institute for Space Studies General Circulation Model – version II’
fvGCM	Global Modeling and Assimilation Office (GMAO) finite-volume GCM
GEOS4-DAS	GEOS Data Assimilation System– version 4
<del>GFDL-AM2</del>	<del>Geophysical Fluid Dynamics Laboratory Global Atmosphere Model</del>
<del>GEOS-Chem-CTM</del>	<del>GEOS-Chem Chemical Transport Model</del>
<del>GEOS3-DAS</del>	<del>GEOS-DAS—version 3</del>
<del>GEOS4-DAS</del>	<del>GEOS-DAS—version 4</del>
<del>GEOS5-DAS</del>	<del>GEOS-DAS—version 5</del>



1  
2  
3  
4  
  
5  
6  
7  
8

Table 2. Characteristics of meteorological data sets used to drive the GMI CTM

Data Set	Number of levels	Top Pressure (hPa)	Vertical Coordinate	Interface Pressure (hPa) <sup>a</sup>	Near-Tropopause Resolution (km)	Bottom layer depth (hPa, m)	Update Period (h)
GEOS1-STRAT	46	0.1	$\sigma$	N/A	~1.0	~12.13hPa, ~100m	6
GISS II'	23	0.002	$\sigma$ -P	150	~1.8-2.5	~24.46hPa, ~200m	3
fvGCM	42 (55 <sup>b</sup> )	0.9 (0.01 <sup>b</sup> )	$\sigma$ -P	200	~1.0	~14.89hPa, ~130m	3
GEOS4	42 (55 <sup>b</sup> )	0.9 (0.01 <sup>b</sup> )	$\sigma$ -P	200	~1.0	~14.89hPa, ~130m	3

<sup>a</sup>The hybrid vertical coordinate consists of sigma ( $\sigma$ ) levels below the interface pressure and constant pressure (P) levels above.

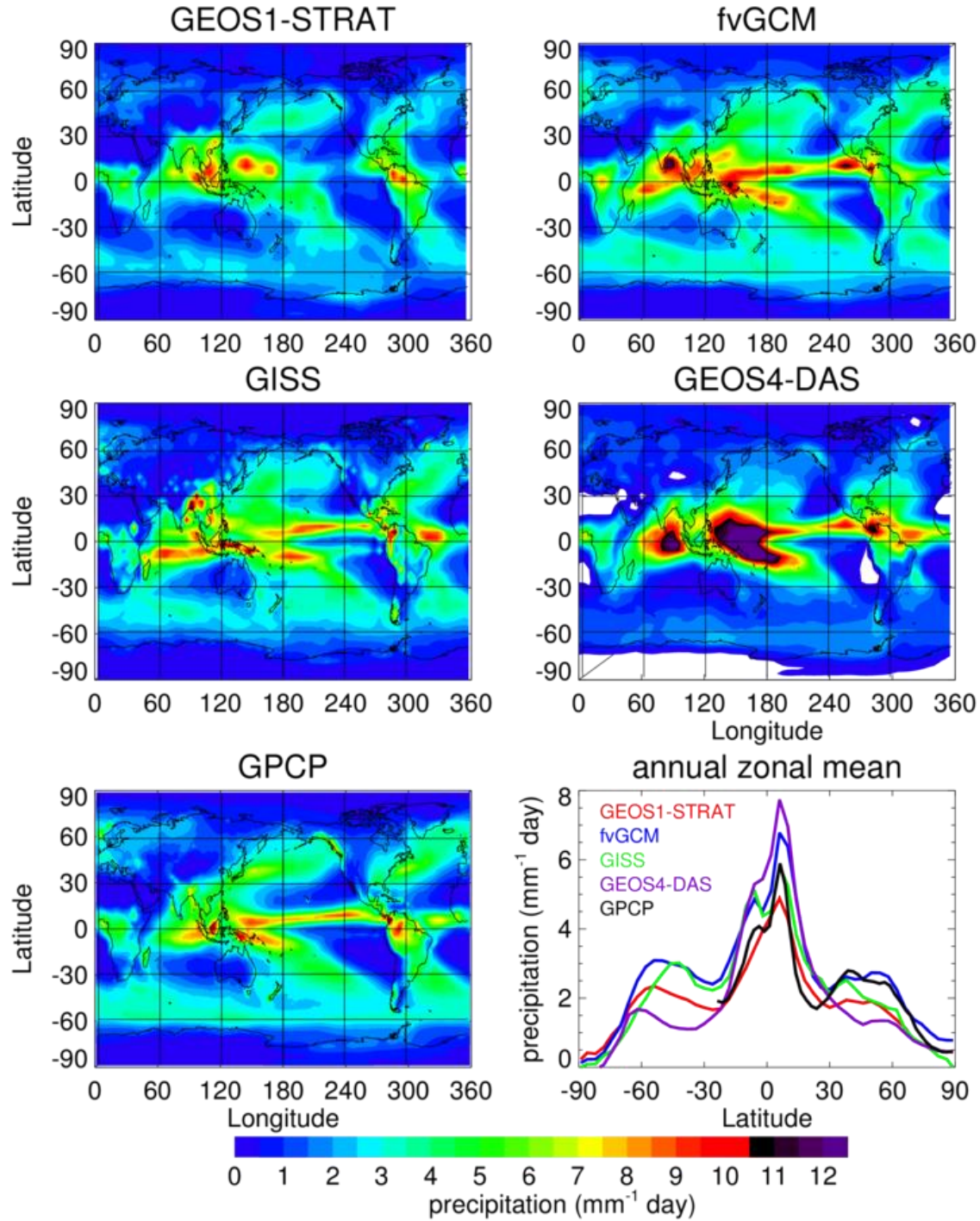
<sup>b</sup>The total number of vertical levels and top level pressure in the original meteorological data set.

Table 3. Annual average global budget of  $^7\text{Be}$  in the model troposphere. The GMI model was driven by the GEOS1-STRAT, GISS II', fvGCM, and GEOS4-DAS meteorological data sets, respectively.

	GEOS1-STRAT	GISS	fvGCM	GEOS4-DAS
Burden, g	4.95 (3.86) <sup>b</sup>	4.00 (3.64) <sup>b</sup>	4.31	4.05
Residence time, days <sup>a</sup>	31 (29)	31 (30)	35	31
Sources, g d <sup>-1</sup>	0.22 (0.18)	0.18 (0.17)	0.18	0.19
STE	0.08 (0.04)	0.05 (0.04)	0.04	0.05
troposphere	0.14 (0.14)	0.13 (0.13)	0.14	0.14
Sinks, g d <sup>-1</sup>	0.22 (0.18)	0.18 (0.17)	0.18	0.19
dry deposition	0.01 (0.01)	0.01 (0.01)	0.01	0.02
wet deposition	0.15 (0.12)	0.12 (0.11)	0.11	0.12
radioactive decay	0.06 (0.05)	0.05 (0.05)	0.06	0.05

<sup>a</sup>Against deposition only. The tropopause was determined in the model using a criterion of 2°C km<sup>-1</sup> lapse rate as defined by World Meteorological Organization. The diagnosed tropopause model layer was included as part of the troposphere.

<sup>b</sup>The numbers in the brackets indicate the values when  $^7\text{Be}$  cross-tropopause fluxes were adjusted for GMI/GEOS1-STRAT and GMI/GISS. See text for details.



2

3 Figure 1. Annual mean total precipitation (mm day<sup>-1</sup>) at the surface in the GEOS1-STRAT, GISS  
 4 II', fvGCM, and GEOS4-DAS meteorological data sets and in the observational data set from the  
 5 Global Precipitation Climatology Project (GPCP, 1979-2009). Also shown is the annual zonal  
 6 mean precipitation (bottom right panel).

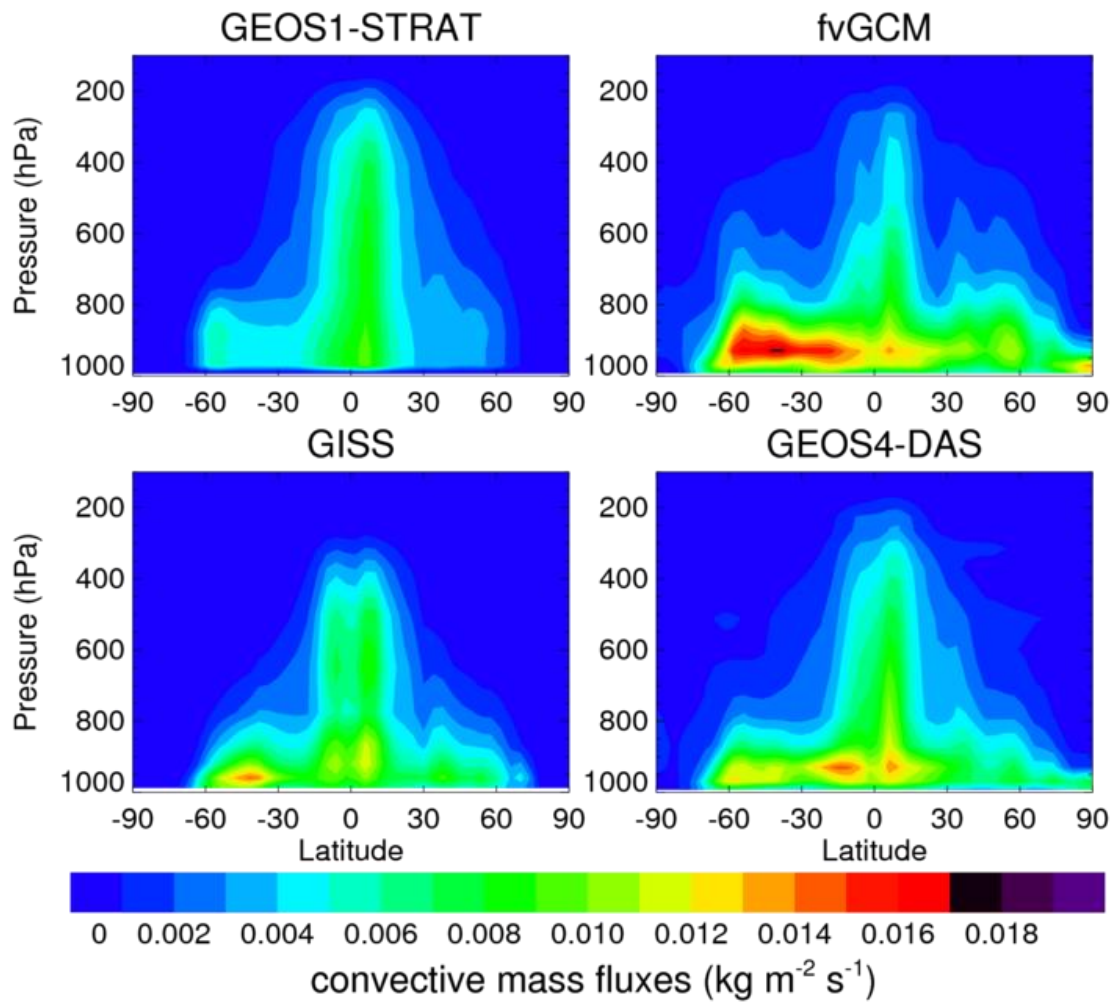


Figure 2. Annual zonal mean convective mass fluxes ( $\text{kg m}^{-2} \text{s}^{-1}$ ) in the GEOS1-STRAT, GISS II' GCM, fvGCM, and GEOS4-DAS meteorological data sets.

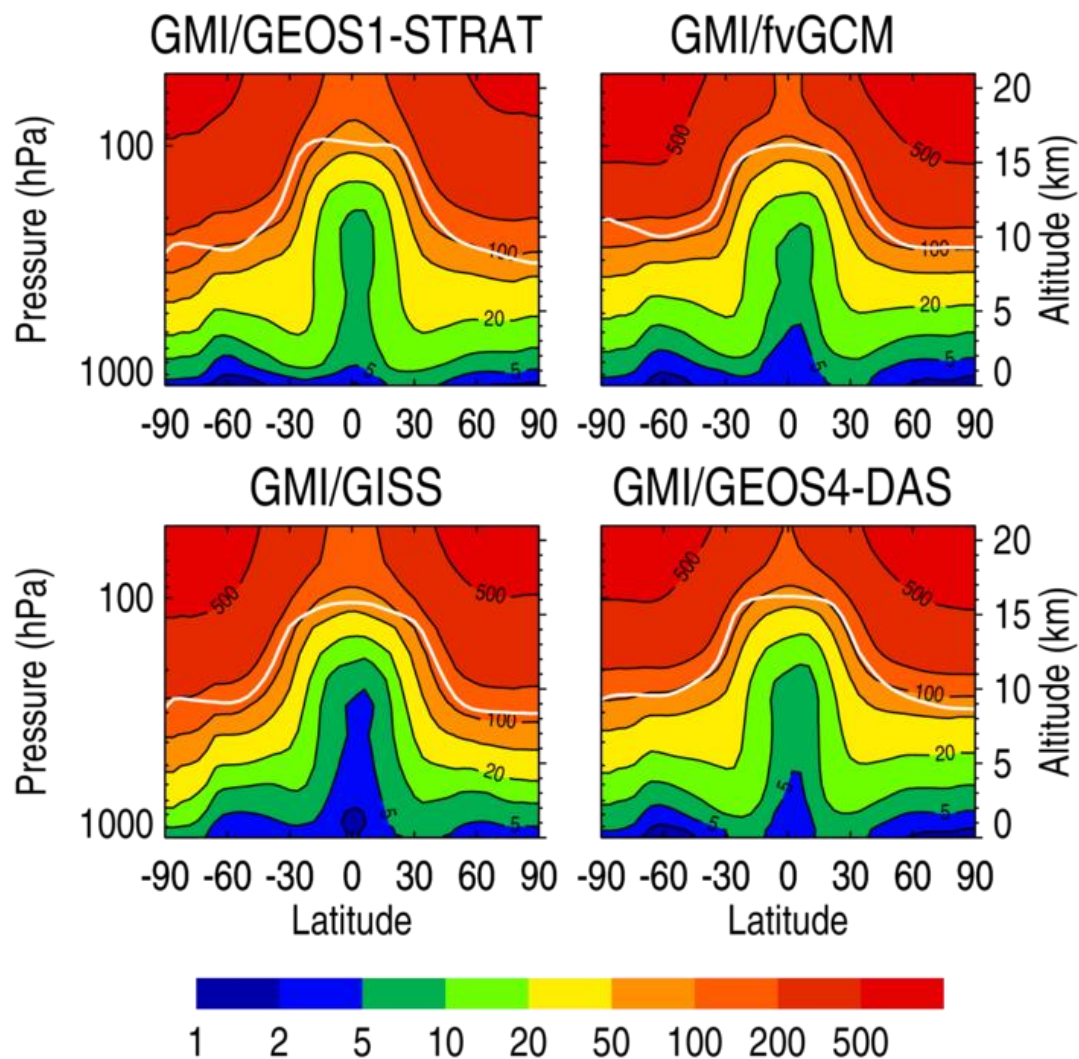


Figure 3. Annual zonal mean mixing ratios (mBq/SCM) of  $^7\text{Be}$  as a function of latitude and pressure (altitude), as simulated by the standard GMI CTM. The white lines indicate the annual average thermal tropopause height. Contour levels are 2, 5, 10, 20, 50, 100, 200, 500 mBq/SCM.

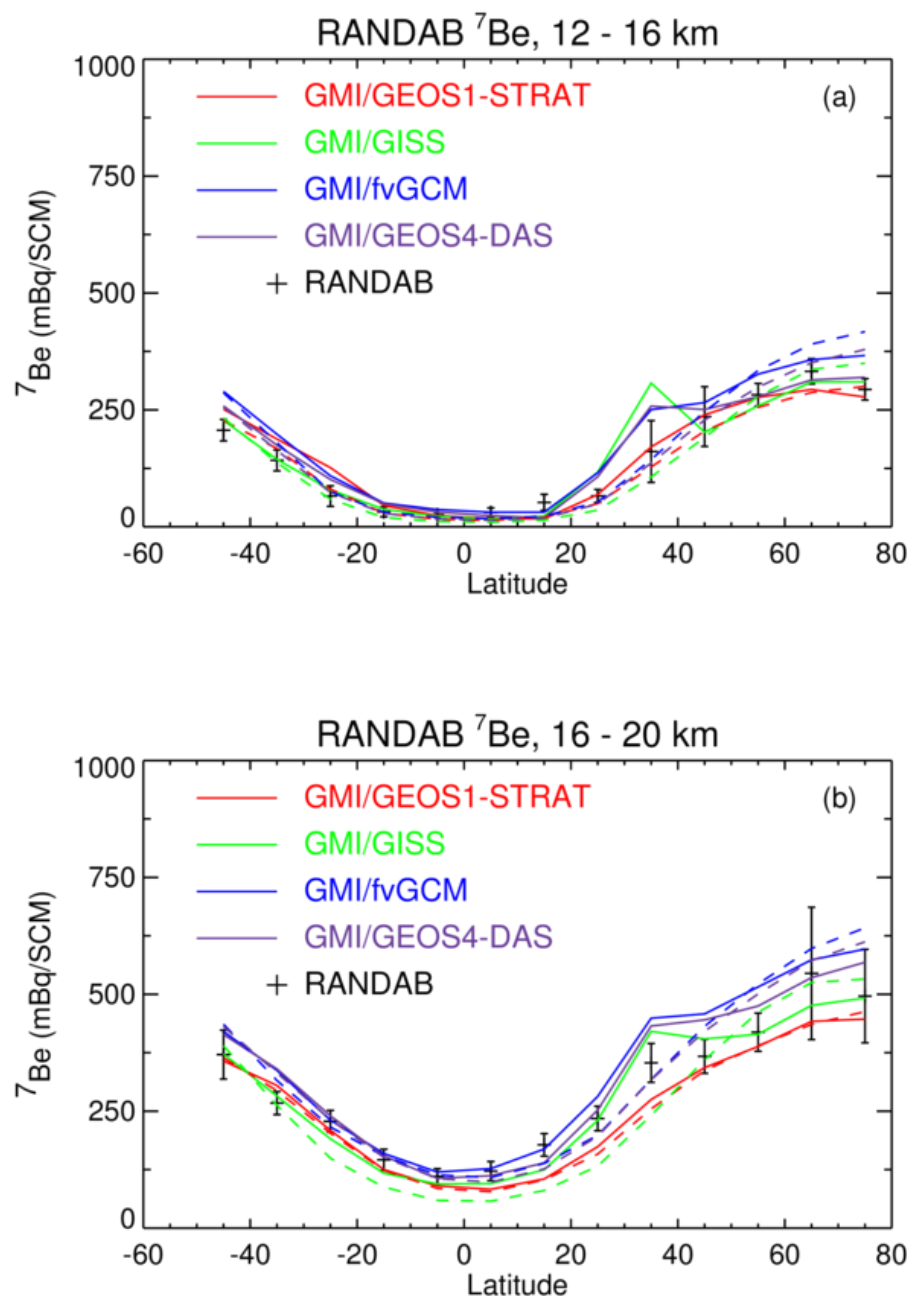
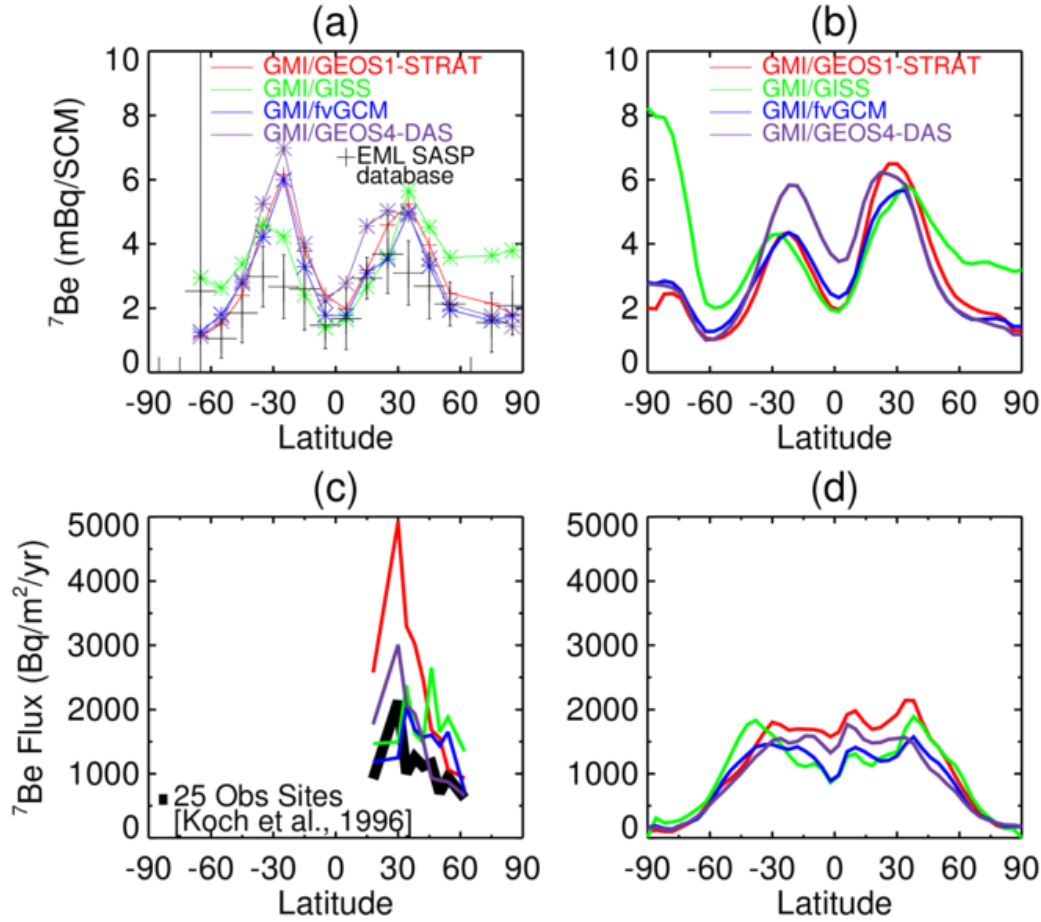


Figure 4. Observed and simulated latitudinal distributions of  $^7\text{Be}$  in the (a) 12-16km and (b) 16-20km regions. Observed data from the EML RANDAB database are averaged into  $10^\circ$  bins, following Considine et al. (2005). Error bars represent  $\pm 2$  times the standard error of the averages. Model results are sampled at observation locations and month. Also shown as dashed lines are model zonal mean  $^7\text{Be}$  concentrations to show the global representativeness of the averages constructed from sampling the simulations at the observation locations.





2

3

Figure 5. (a). Observed and simulated latitudinal distributions of  $^7\text{Be}$  concentrations (mBq/SCM) near the surface.  $^7\text{Be}$  cross-tropopause fluxes were not adjusted for the GMI/GEOS1-STRAT and GMI/GISS simulations (see Section 3). Observed data from the EML Surface Air Sampling Program (SASP) database are averaged into 10° bins. Those sites with elevation higher than 500m are not included. Error bars represent  $\pm 2$  times the standard error of the averages. Model results are sampled at observation locations and month. (b). GMI simulated annual zonal mean concentrations of  $^7\text{Be}$  (mBq/SCM) near the surface. (c). Observed (black) and GMI simulated (color) annual mean total deposition fluxes (Bq/m<sup>2</sup>/yr) of  $^7\text{Be}$  (at 25 sites) as a function of latitude. The data from individual sites are averaged over 4° latitude bins. The model is sampled at observation locations. (d). GMI simulated annual zonal mean total deposition fluxes (Bq/m<sup>2</sup>/yr) of  $^7\text{Be}$ .

15

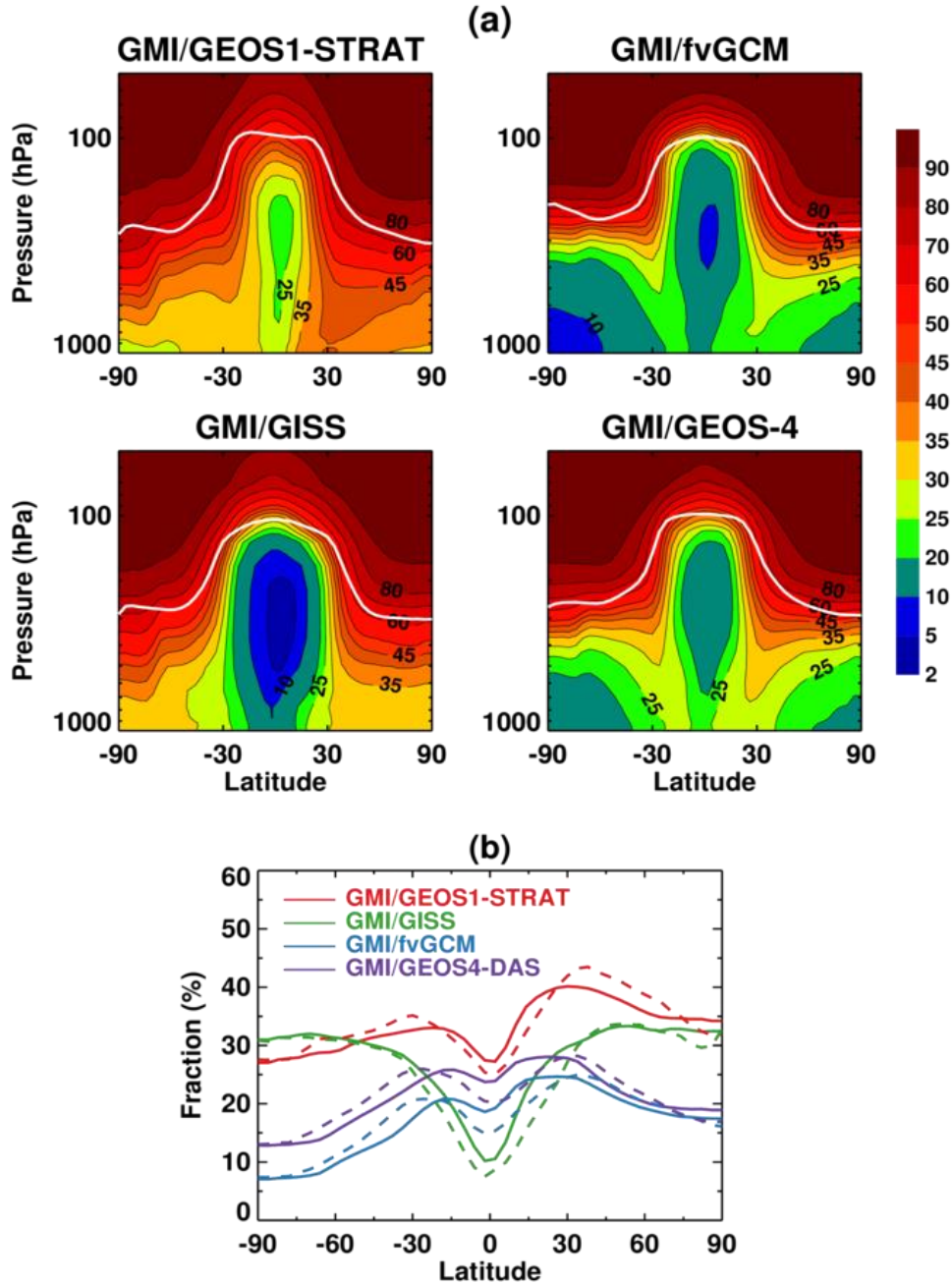


Figure 6. (a). Stratospheric fraction (%) of annual zonal mean ~~tropospheric-atmospheric~~  $^7\text{Be}$  concentrations in the ~~standard~~-model simulations as a function of latitude and pressure. ~~Values are annual averages.~~ The white lines indicate thermal tropopause height. Contour levels are 5, 10, 20, 25, 30, 35, 40, 45, 50, 60, 70, 80, 90%. (b). Stratospheric fraction of annual zonal mean surface  $^7\text{Be}$  concentrations (solid lines) and that of annual zonal mean  $^7\text{Be}$  total deposition fluxes (dashed lines) in the ~~standard-model~~ simulations as a function of latitude. ~~Values are annual averages.~~



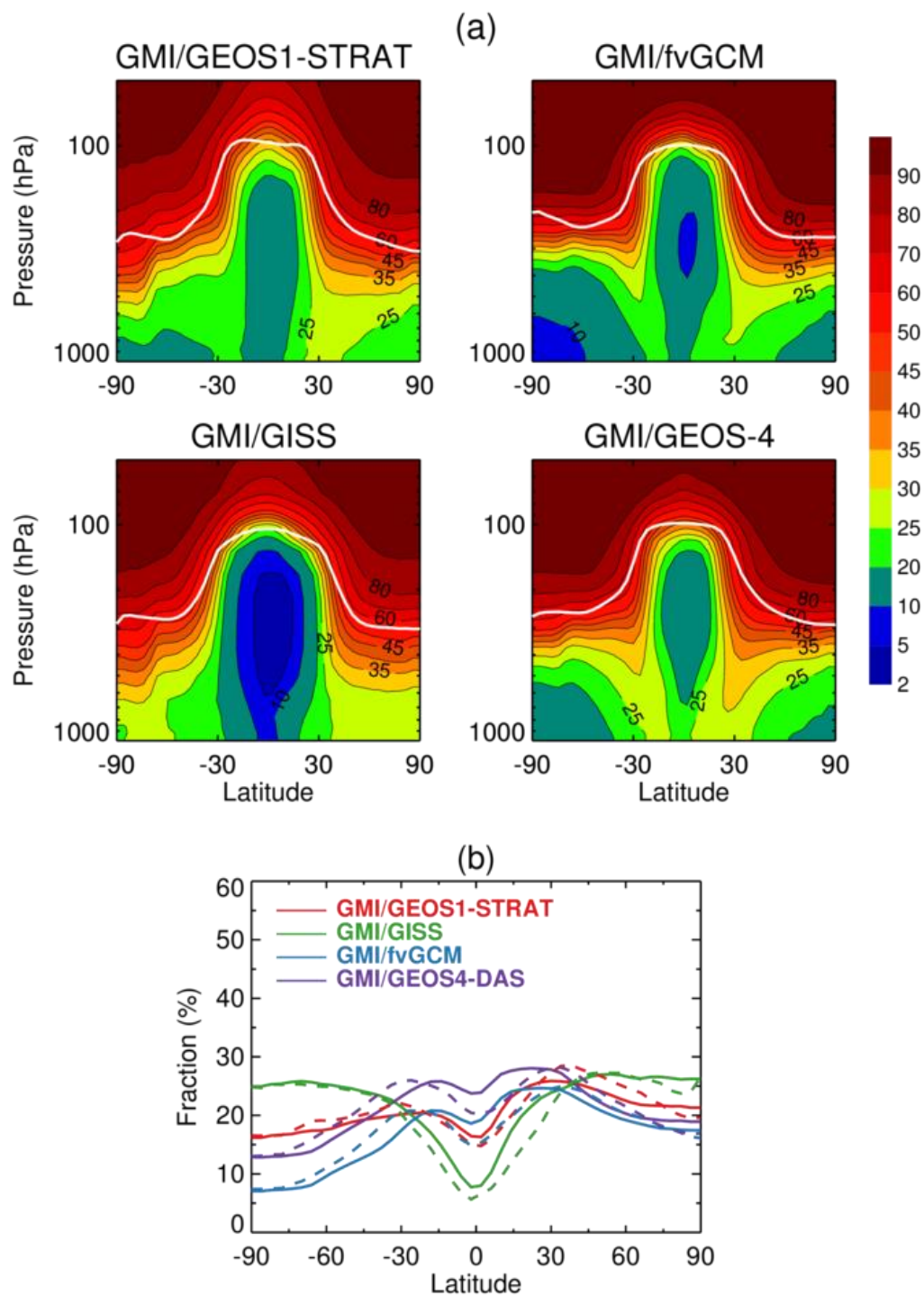
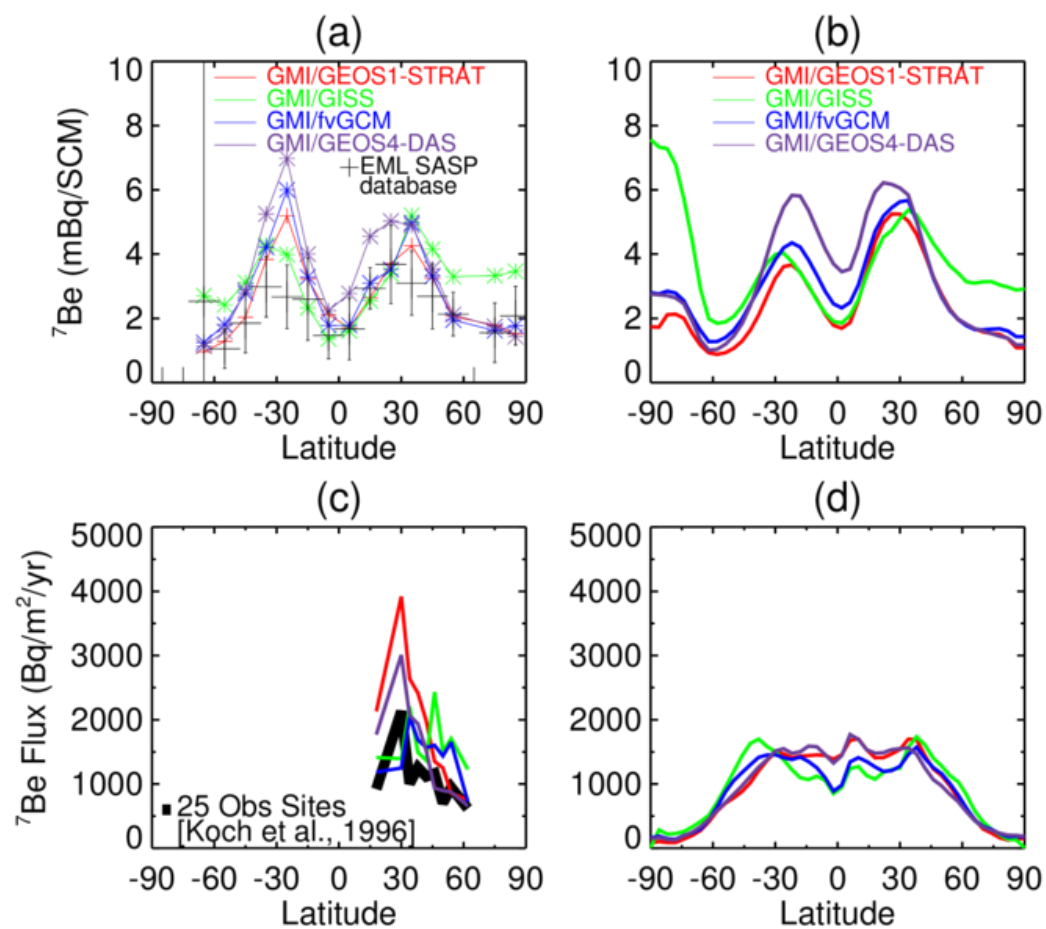


Figure 7. Same as Figure 46, except that  $^7\text{Be}$  cross-tropopause fluxes have been adjusted for GMI/GEOS1-STRAT and GMI/GISS.

1



2

3

4

5 Figure 8. Same as Figure 5, except that  $^7\text{Be}$  cross-tropopause fluxes have been adjusted for  
 6 GMI/GEOS1-STRAT and GMI/GISS.

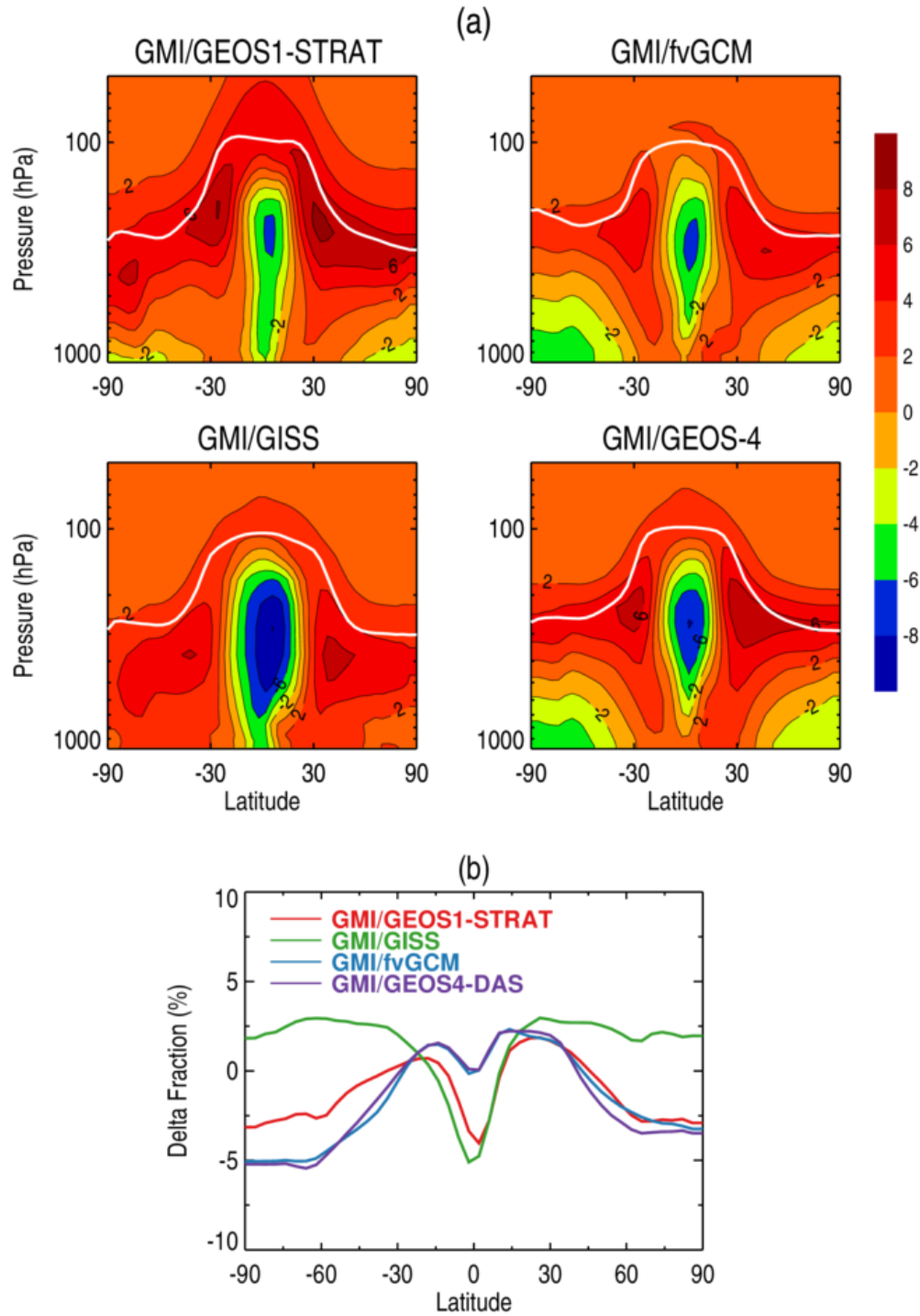


Figure 9. Same as Figure 6(a,b), except for the differences in the stratospheric fraction (%) of zonal mean ~~tropospheric-atmospheric~~ <sup>7</sup>Be concentrations between the standard simulation and a simulation where wet scavenging is turned off. Contour levels are -8, -6, -4, -2, 0, 2, 4, 6, 8%.

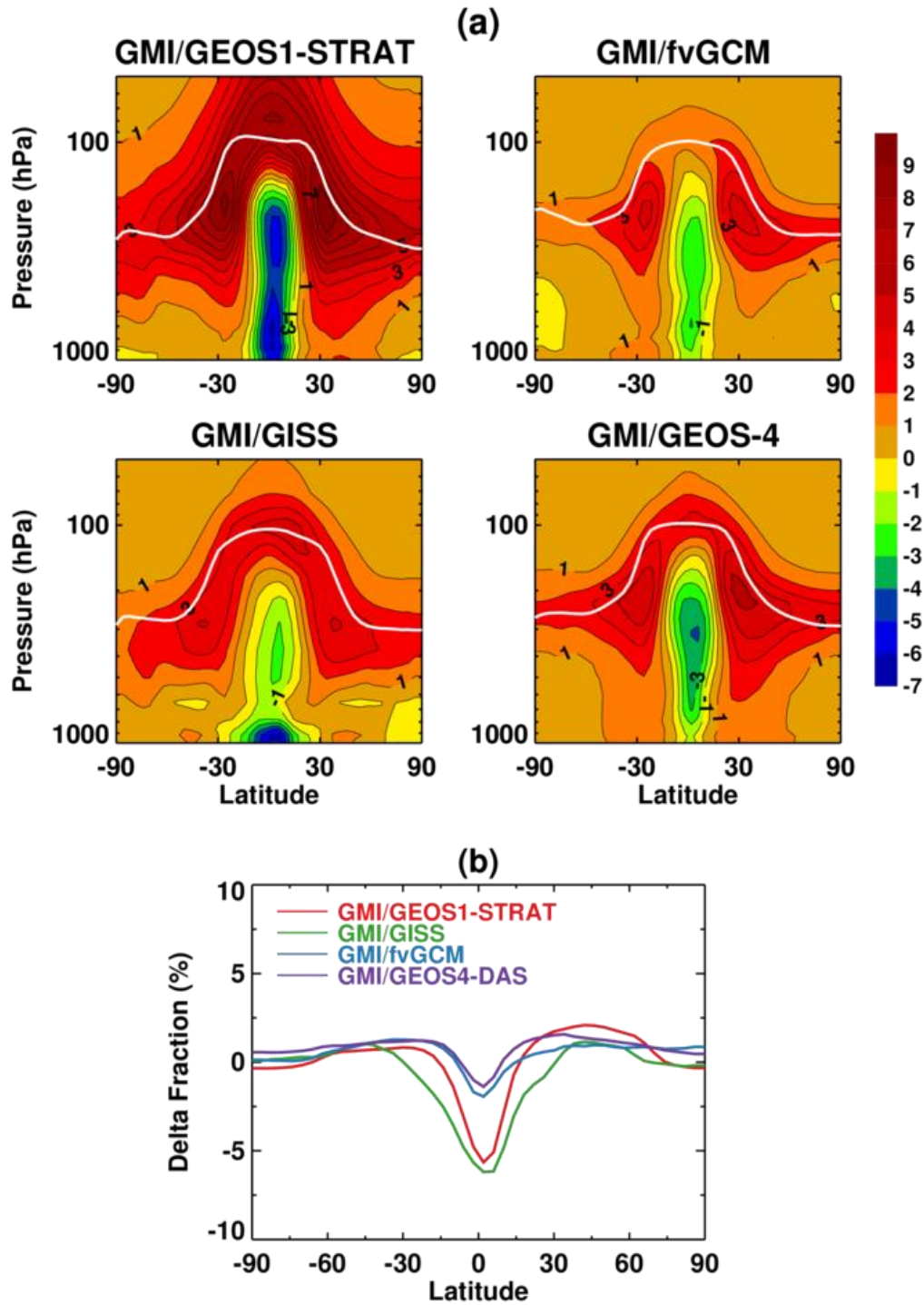


Figure 10. Same as Figure 6 (a,b), except for the differences in the stratospheric fraction (%) of zonal mean ~~tropospheric-atmospheric~~ <sup>7</sup>Be concentrations between the standard simulation and a simulation where convective transport and scavenging are turned off. Contour levels are -4, -3, -2, -1, 0, 1, 2, 3, 4%.

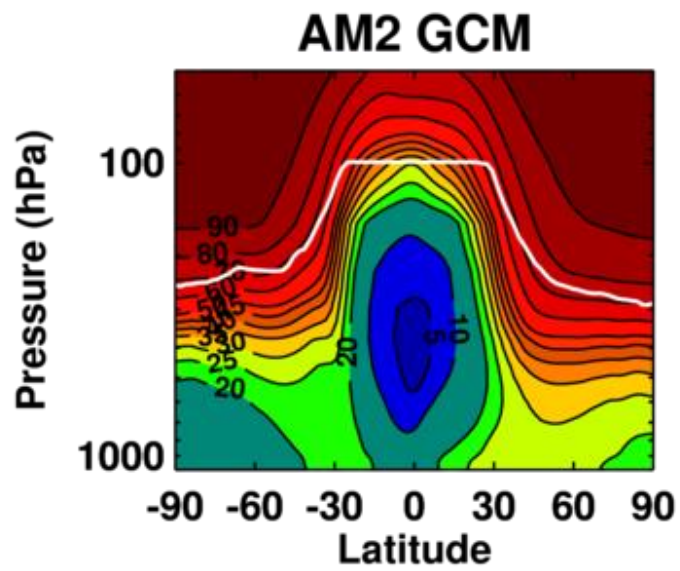


Figure 11. Same as Figure 6a, except for AM2 GCM (year 1987).

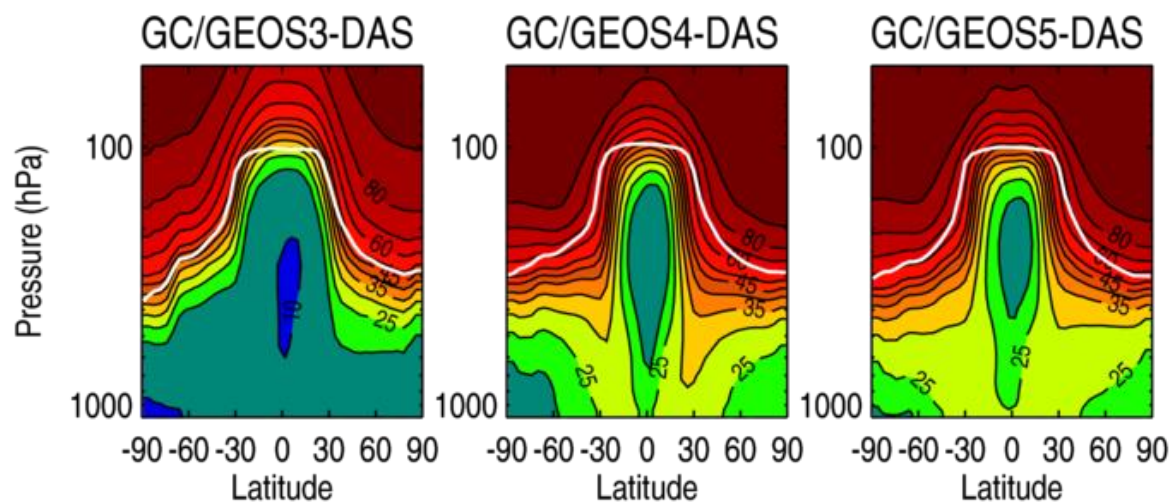


Figure 12. Same as Figure 6a, except that the GEOS Chem model was driven with the GEOS3-DAS (2001), GEOS4-DAS (2004), and GEOS5-DAS (2004) meteorological fields.

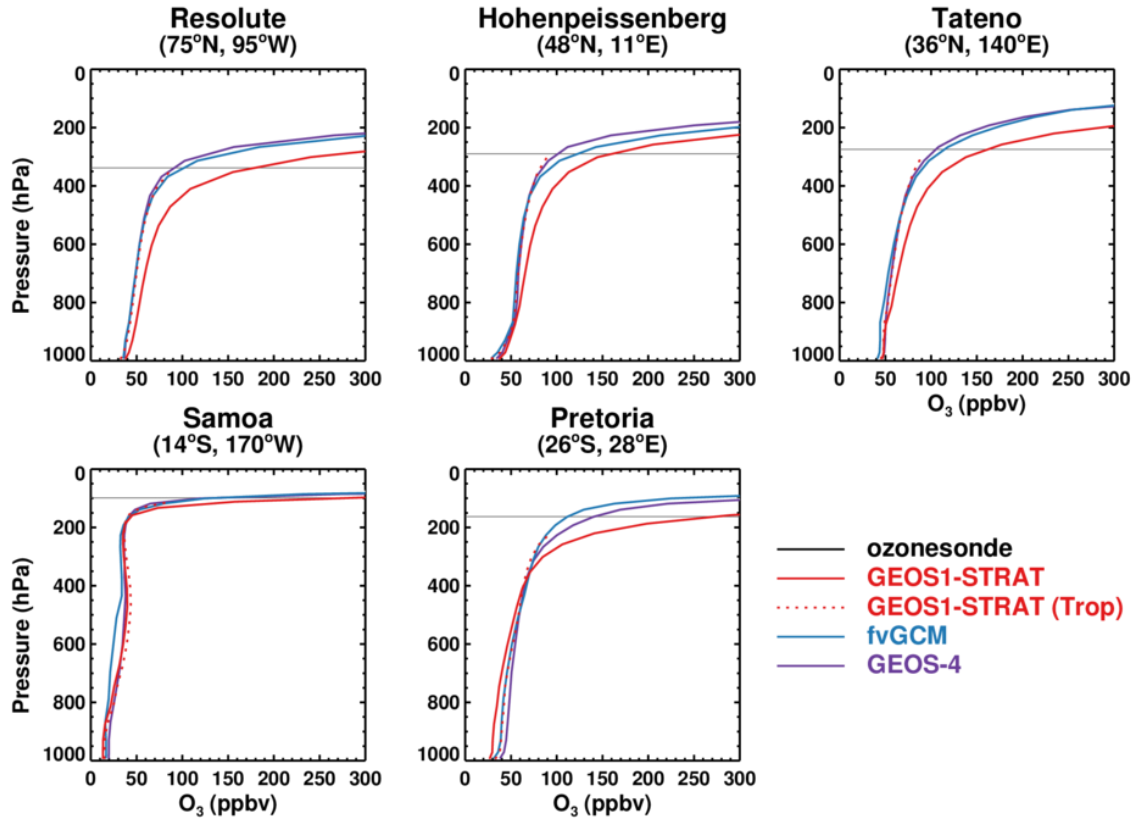


Figure 1311. Comparisons of GMI simulated tropospheric ozone profiles (color lines) with ozonesonde observations (black line) for a range of latitudes. Values are annual averages. Solid color lines indicate the GMI simulations. Also shown as dotted lines are tropospheric ozone profiles as simulated by the GMI tropospheric model driven by the GEOS1-STRAT meteorological field. The horizontal grey line indicates the approximate location of tropopause (i.e., the pressure level corresponding to 100 ppbv ozone concentrations in the ozonesonde observations).



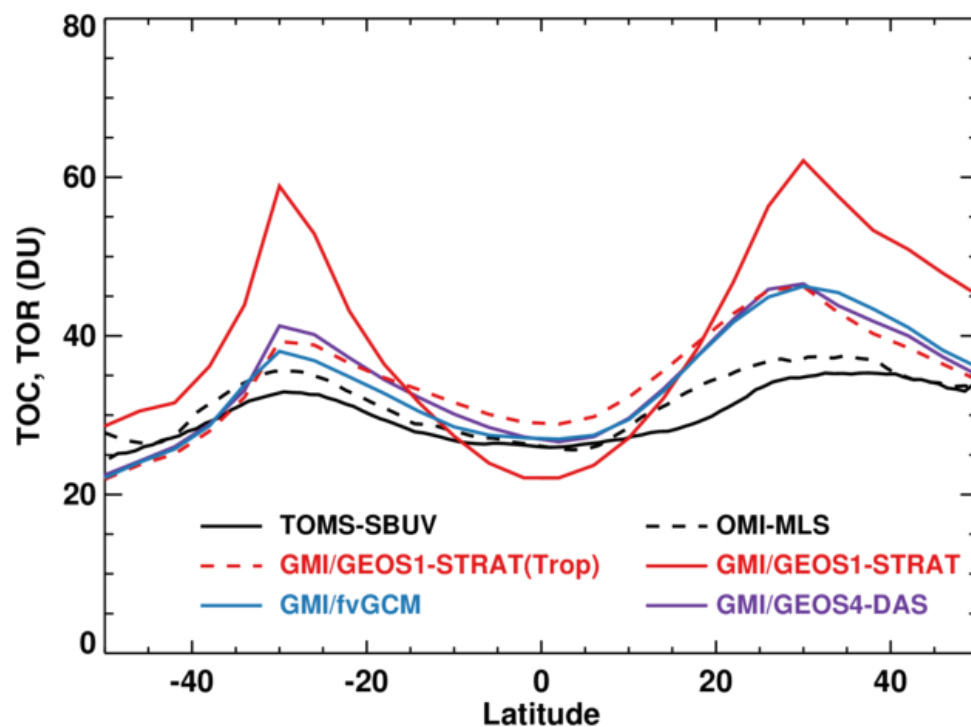


Figure 14.12. GMI simulated annual zonal mean tropospheric ozone column (TOC in Dobson Units) compared with observed tropospheric ozone residuals from TOMS/SBUV (1979-2005 average) and OMI/MLS (October 2004 - July 2008 average). Also shown is the annual zonal mean TOC simulated by the tropospheric version of the GMI model.



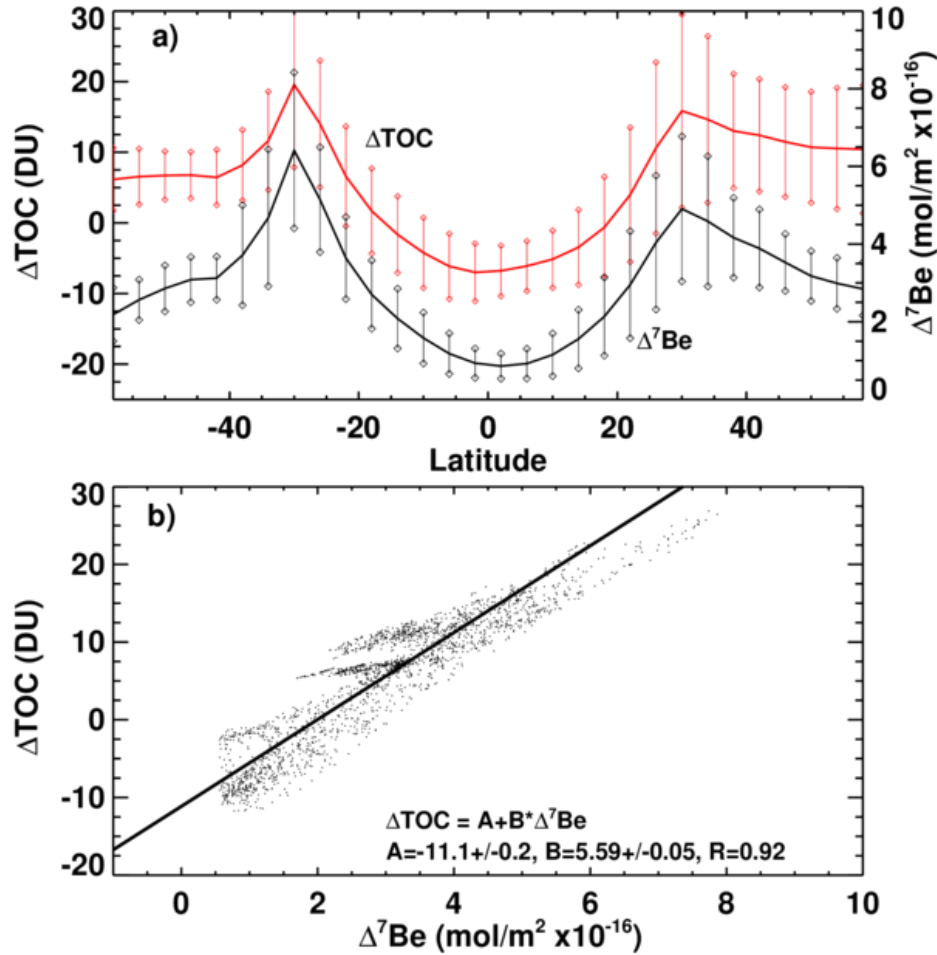


Figure 1513. (a). Latitudinal variations of annual zonal mean  $^7\text{Be}$  overestimate ( $\Delta^7\text{Be}$ ) and tropospheric ozone column overestimate ( $\Delta\text{TOC}$ ) as simulated by GMI/GEOS1-STRAT. Error bars represent  $\pm 2$  times the standard error of the averages. (b). the correlation between the global distributions of  $\Delta^7\text{Be}$  and  $\Delta\text{TOC}$ . The lines of best fit are calculated using the reduced-major-axis (RMA) method (Hirsch and Gilroy, 1984). See text for details.